Numerical modelling of autogenous shrinkage of rice husk ash blended cement mortar

Lu, Tianshi; Yang, Han; Huang, Hao; Zhao, Xiang

DOI
10.1680/jadcr.24.00078

Publication date
2024

Document Version
Accepted author manuscript

Published in
Advances in Cement Research

Accepted manuscript doi:
10.1680/jadcr.24.00078

Accepted manuscript doi:
10.1680/jadcr.24.00078

Submitted: 3 May 2024

Published online in 'accepted manuscript' format: 18 September 2024

Manuscript title: Numerical modelling of autogenous shrinkage of rice husk ash blended cement mortar

Authors: Tianshi Lu[1,3], Han Yang[1], Hao Huang[2,3] and Xiang Zhao[1]

Affiliations: [1]School of Civil Engineering and Geomatics, Southwest Petroleum University, Chengdu, China, [2]School of Civil Engineering, Hubei Engineering University, Xiaogan, China, [3]Department of Materials, Mechanics, Management & Design, Faculty of Civil Engineering and Geoscience, Delft University of Technology, Delft, the Netherlands

Corresponding author: Hao Huang, School of Civil Engineering and Geomatics, Southwest Petroleum University, Chengdu, China

E-mail: h.huang@hbeu.edu.cn

Accepted manuscript doi:
10.1680/jadcr.24.00078

Abstract

Addition of rice husk ash (RHA) is an effective internal curing method to mitigate self-desiccation and autogenous shrinkage of hydrating cementitious materials. Although a certain number of experimental researches on this topic have been carried out, a comprehensive study about numerical simulation of mitigating effect of RHA on autogenous shrinkage of cementitious materials is still scarce. In this study, a numerical model of autogenous shrinkage of rice husk ash blended cement mortar was proposed. The proposed numerical model was based on Pickett model and improved by taking visco-elastic behaviour of rice husk ash blended cementitious materials into account. Final setting time, chemically bound water, compressive strength, internal relative humidity (RH) and autogenous shrinkage of pure Portland cementitious materials and rice husk ash blended cementitious materials were experimentally studied. Liquid absorption capacity and water vapour desorption isotherm of rice husk ash were also measured. The comparison between the simulated and measured autogenous shrinkage showed that the autogenous shrinkage of rice husk ash blended cement mortar can be predicted accurately with the proposed numerical model.

Keywords: rice husk ash, restraining effect, creep, simulation, cement paste and mortar, UN SDG 9

Accepted manuscript doi:
10.1680/jadcr.24.00078

Introduction

Ultra-high performance concrete (UHPC) is an advanced cementitious material with high strength and excellent durability. It is typically made by Portland cement, supplementary materials, fine sand, high-strength steel fibre, water reducers and water (Schmidt and Fehling, 2005). Although UHPC has been widely used in civil engineering due to its numerous advantages, there are still some drawbacks of this promising building material, e.g., cracking (Fehling et al., 2014). Aggressive agents may penetrate through cracks and lead to concrete deterioration (Wang et al., 2022). One of the main reasons for cracking is shrinkage. Based on the mechanism, shrinkage of cementitious materials can be divided into several different categories, for example, chemical shrinkage and drying shrinkage (Holt, 2001). As a result of hydration reaction, water content in cementitious materials is expended and relative humidity (RH) drops. This process is self-desiccation (Persson, 1997). Self-desiccation would result in the volume reduction of cementitious materials which is named self-desiccation shrinkage, or autogenous shrinkage (Tazawa, 1999). Generally, water-binder ratio of UHPC is lower than that of ordinary Portland cement concrete. Due to less amount of water, the self-desiccation phenomenon and the autogenous shrinkage of UHPC is more significant (Shen et al., 2018). Therefore, autogenous shrinkage of UHPC has drawn increasing attention during the past few years (Lura, Jensen and Van Breugel, 2003; Lu, Li and van Breugel, 2020; Zhang, Liu and Wang, 2019).

For mitigating the autogenous shrinkage and reducing the cracking potential of UHPC, numerous methods have been proposed during the past few decades, e.g., addition of fibres, increase in volume fraction of aggregate and use of shrinkage reducing agent or expansive agent (Tawfek et al., 2023; Yang, Shi and Wu, 2019; Meddah, Suzuki and Sato, 2011; Jiang et al., 2024; Lu et al., 2023). Among the proposed methods, internal curing is considered as a very effective way to mitigate self-desiccation and autogenous shrinkage of UHPC (Bentz and Jensen, 2004; Geiker, Bentz and Jensen, 2004; Bentz and Weiss, 2011; Wyrzykowski et al., 2011). According to American Concrete Institute (2013), internal curing is defined as supplying water throughout a freshly mixed cementitious mixture by using internal curing agent which is able to release water as needed for hydration and to compensate moisture lost through evaporation or self-desiccation. There are different kinds of internal curing agents, e.g., lightweight aggregate and super-absorbent polymers (SAPs) (Gifta, Prabavathy and Kumar, 2013). But due to its negative effect on mechanical behaviours, light-weight aggregate is not always applicable in UHPC. SAPs are the most frequently used internal curing agent in practice (SAP, 2012). SAPs are polymeric materials with the ability to absorb liquid and keep the liquid within their pore structure (SAP, 2012). There are different types of SAPs with various sizes and shapes. The most commonly used commercial SAPs products are covalently cross-linked polyacrylates and copolymerized polyacrylamides (Jensen and Hansen, 2001). It was reported that the autogenous shrinkage of concrete at the age of 7 days will be significantly decreased by adding the commercially available super-absorbent polymers (Mechtcherine, Dudziak and Hempel, 2009.). Although the autogenous shrinkage can be effectively mitigated with the addition of SAPs, there are still some disadvantages. For

Accepted manuscript doi:
10.1680/jadcr.24.00078

example, the addition of SAPs will result in voids in the cement matrix of UHPC, which are harmful to the mechanical properties of UHPC (Justs et al., 2015).

During the past few decades, researchers were still trying to find an alternative internal curing agent of UHPC. Among numerous alternative options, rice husk ash is considered as a potential internal curing agent to be used in UHPC due to its pozzolanic reactivity and porous structure. When rice husk is incinerated completely, the residue after combustion is called rice husk ash (abbreviated as RHA) (Boateng and Skeete, 1990; Della, Kühn and Hotza, 2002). The main component of RHA is amorphous silica (90-96 wt%) (Chandrasekhar et al., 2003; Van Tuan et al., 2011). Van Tuan et al. (Van Tuan et al., 2011; Kang, Hong and Moon, 2019; Vieira et al., 2020) reported that the pore volume of RHA is bigger than that of most pozzolanic materials with similar particle sizes. Due to its high porosity, RHA can be used as a water reservoir and provide internal curing for UHPC.

In recent years, a lot of researches about the autogenous shrinkage of RHA cement paste, mortar and concrete have been carried out (de Sensale, Ribeiro and Gonçalves, 2008; Van Tuan, Ye and van Breugel, 2010; Amin et al., 2019; Vieira et al., 2022; Li et al., 2023). According to these researches, the autogenous shrinkage of RHA cementitious materials will be markedly reduced due to the internal curing effect of RHA. Although previous researches confirmed the effectiveness of rice husk ash on mitigating autogenous shrinkage, most of them are still limited to experimental study. A numerical study about the autogenous shrinkage of RHA cement paste, mortar and concrete is still scarce. Cement mortar and concrete are mainly made up by two separate parts, i.e., shrinking cement matrix and non-shrinking aggregate. Non-shrinking aggregate will restrain the deformation of cement matrix (Pickett, 1956; Holt, 2002). An experimental and numerical study about the effects of RHA on mechanical properties and internal relative humidity of cement paste together with restraining effect of aggregate on autogenous shrinkage of UHPC will be very useful.

Since the 1950s, different numerical models have been proposed to simulate the restraining effect of aggregate on the deformation of concrete, e.g., series model and parallel model (Hansen and Nielsen, 1965; Hobbs, 1974). There are common assumptions of these proposed model. First, concrete is made up by two homogenous parts, i.e., cement matrix and aggregate. Second, both cement matrix and aggregate are assumed to be elastic material and creep is not taken into consideration. Third, the influence of microcracking on the elastic properties of cement matrix is neglected. Deformation of concrete only depends on the deformation of cement matrix and the aggregate volume fraction. According to literature (Li et al., 2021), the shrinkage of concrete can be approximated by using these proposed models. However, there are always significant deviations between the simulated autogenous shrinkage with the proposed models and measured results. Some researchers attributed these deviations to the neglect of the visco-elastic behaviour of the cementitious materials, which also named as creep (Li et al., 2021; Grasley et al., 2005).

In this paper, a numerical model is proposed to predict the autogenous shrinkage of Portland cement mortar and rice husk ash blended cement mortar. The proposed model is based on Pickett model (Pickett, 1956) and improved. In the improved Pickett model, the visco-elastic

behaviour of rice husk ash blended cementitious materials, i.e., creep, is taken into consideration. The predicted autogenous shrinkage of cement mortars is contrasted with the experimental results to assess the accuracy of prediction. Portland cement paste (CEM I 52.5N) and two types of RHA cement paste are considered. The weight ratios of rice husk ash in the two types of RHA cement paste are 10% and 20%, respectively. Two kinds of cement mortar with and without addition of RHA are also investigated. The RHA-binder weight ratio of RHA cement mortar is 20%. The sand-binder weight ratios of all cement mortars are 1. Water-binder ratios of all mixtures are 0.25. Apart from autogenous shrinkage, influence of rice husk ash on the mechanical proprieties, relative humidity and hydration process of cement mixtures is also experimentally studied in this paper.

1. Numerical model of autogenous shrinkage

During the past few decades, many numerical models have been used to predict the deformation of cement mortar and concrete, e.g., parallel model, series model and Hobb's model (Hansen and Nielsen, 1965; Hobbs, 1974). In these models, the deformation of cement mortar and concrete is calculated as a function of the sand/aggregate volume concentration and the autogenous shrinkage of the cement matrix. In this study, a numerical model proposed by Pickett (1956), which has been widely used by researchers (Hammer and Sellevold, 2004; Grasley, 2006; Wei, 2008), is adopted and improved to predict the autogenous shrinkage of Portland and RHA cement mortar.

2.1 Theoretical basis of Pickett model

In Pickett model, cement mortar or concrete is made up by two components, i.e., cement matrix and solid particles which are sand or aggregate. The solid particle and cement matrix are represented as a small sphere and a homogenous shell surrounding the sphere as shown in Fig. 1. During the hydration process, the surrounding cement matrix, which is usually cement paste, will shrink and inner solid particles will restrain the shrinkage of the cement matrix. In order to predict the shrinkage of cement mortar or concrete, the influence of one solid particle on the shrinking cement matrix is considered first.

Due to the restraint of inner solid particle, a normal stress perpendicular to the radius σ_t and a normal stress in the radial direction σ_r will generate in cement matrix as shown in Fig. 1 (Timoshenko and Goodier, 1951):

$$\sigma_t = \frac{p\mathrm{a}^3}{2r^3}\frac{b^3+2r^3}{b^3-\mathrm{a}^3} \tag{1}$$

$$\sigma_r = -\frac{p\mathrm{a}^3}{r^3}\frac{b^3-r^3}{b^3-\mathrm{a}^3} \tag{2}$$

where σ_t [MPa] is the normal stress perpendicular to the radius; p [MPa] is the unit pressure between inner solid particle and outer cement matrix; r [m] is the radial coordinate; a [m] is

Accepted manuscript doi:
10.1680/jadcr.24.00078

the radius of inner solid particle; b [m] is the radius of cement matrix shell; σ_r [MPa] is the normal stress in the radial direction.

As shown in Fig. 2a, the shrinking volume of cement matrix without restraint is:

$$4\pi b^2\delta = 4\pi b^2\varepsilon b = 3\varepsilon V \quad (3)$$

where ε [m/m] is the unit linear deformation, i.e., δ/b; V [m^3] is the volume of the cement matrix, i.e., $4\pi b^3/3$.

Due to the restraint of inner solid particle, the shrinkage of the outer cement matrix will be reduced. Reduction of the shrinkage can be expressed as (Fig. 2b):

$$\delta_r = \frac{r}{E_p}[(1-\vartheta_p)\sigma_t - \vartheta_p\sigma_r] \quad (4)$$

where ϑ_p [-] and E_p [MPa] are the Poisson ratio and Young's modulus of the cement matrix.

Therefore, the reduced shrinking volume of the cement matrix caused by one solid particle is:

$$4\pi b^2\delta_r = \frac{3pV_s}{E_p}\left(\frac{1-\vartheta_p}{2}\right)\frac{3b^3}{b^3-\mathrm{a}^3} = 3\Delta\varepsilon V \quad (5)$$

where $V_s = 4\pi\mathrm{a}^3/3$ is the volume of inner solid particle; $\Delta\varepsilon$ [m/m] is the reduction in the unit linear deformation, i.e., δ_r/b.

Meanwhile, pressure between inner solid particle and outer cement matrix p causes a volume reduction of inner solid particle (Fig. 2b). The volume reduction of inner solid particle is:

$$\frac{3(1-2\vartheta_s)pV_s}{E_s} = 3\varepsilon V_s - 4\pi\mathrm{a}^2\delta_r \quad (6)$$

where ϑ_s [-] is the Poisson ratio of inner solid particle and its value is taken as 0.25 in this study [47]; E_s [MPa] is Young's modulus of inner solid particle and its value is taken as 70 MPa (Lura, 2003).

Eliminating p from Equation 5 and 6 gives:

$$\Delta\varepsilon V = \beta\varepsilon V_s \quad (7)$$

where

$$\beta = \frac{3(1-\vartheta_p)}{1+\vartheta_p+2(1-\vartheta_s)E_p/E_s} \quad (8)$$

In Equation 7, the restraint of one solid particle on shrinking cement matrix is described. If the sand/aggregate volume ratio of cement mortar is Φ_A [-], the relationship between the shrinkage of cement mortar and corresponding cement paste is (Pickett, 1956):

$$\varepsilon_m = \varepsilon_p(1-\Phi_A)^\beta \quad (9)$$

where ε_m [m/m] and ε_p [m/m] are the shrinkage of cement mortar and corresponding cement paste.

Accepted manuscript doi:
10.1680/jadcr.24.00078

2.2 Improved Pickett model

Although Pickett model has been widely used to predict the autogenous shrinkage of cement mortar and concrete, there is always discrepancy between the measured and predicted results, especially for the mixtures with low water-biner ratio and high sand/aggregate volume ratio (Wei, 2008). There are several causes of the discrepancy, e.g., micro-cracking and creep. Cement matrix is a kind of visco-elastic material. There are two constituent components of the deformation of cement matrix, i.e., an elastic part and creep. The deformation of cement matrix can be calculated as:

$$\varepsilon_p(t) = \varepsilon_e(t) + \varepsilon_c(t) \tag{10}$$

where $\varepsilon_p(t)$ [m/m] is the total deformation at time t; $\varepsilon_e(t)$ [m/m] is the elastic deformation and $\varepsilon_c(t)$ [m/m] is the creep at time t.

Calculation of elastic deformation $\varepsilon_e(t)$ is based on Hooke's law:

$$\varepsilon_e(t) = \frac{\sigma(t)}{E_p(t)} \tag{11}$$

where $\sigma(t)$ [MPa] and $E_p(t)$ [MPa] are the applied stress and Young's modulus of cement matrix at time t.

Creep is the increased strain or deformation of a material under a constant load. During the past few decades, a lot of numerical models have been proposed by researchers to simulate the creep of cementitious materials (Klug and Wittmann, 1974; Bažant and Osman, 1976; Van Breugel, 1980; Bažant and Chern, 1985; Delsaute, Torrenti, and Staquet, 2017). Among these proposed numerical models, solidification model which was proposed by Bažant has been widely used and developed to simulate the creep of hardening cementitious materials (Bazant and Prasannan, 1989a; Bazant and Prasannan, 1989b; Hedegaard, 2020; Mabrouk, Ishida and Maekawa, 2004). In this study, a developed solidification model which was proposed by Hedegaard (Hedegaard, 2020) is used to describe the visco-elastic behavior of cement matrix. In this model, creep is calculated as a function of creep compliance and load:

$$\varepsilon_c(t) = J(t, t_0)\sigma(t_0) \tag{12}$$

where t_0 [days] is the time when the load is applied; $\sigma(t_0)$ [MPa] is the applied load; $J(t, t_0)$ [MPa^{-1}] is the creep compliance which is expressed as:

$$J(t, t_0) = \frac{1}{E_i} + \left(\frac{P_1}{K}\right)\left(\frac{1}{t_0 - \beta}\right) ln\left[\frac{t_0}{t}\left(\frac{t - t_0}{\beta} + 1\right)\right] + P_1\, ln\left(\frac{t - t_0}{\beta} + 1\right) + \left(\frac{P_2}{K t_0}\right)\left(\frac{t - t_0}{t}\right) + P_2\, ln\frac{t}{t_0} \tag{13}$$

where E_i [MPa] is the instantaneous modulus which is 1.43 times that of Young's modulus E_p; P_1 [MPa^{-1}] is named as the viscoelastic compliance which is a function of compressive strength f_c; β [days] is the time constant, 2×10^{-5}; P_2 [MPa^{-1}] is named as the flow constant, 0.7×10^{-5}; K [days^{-1}] is the rate constant, 0.5. More details of these parameters can be found in literature (Hedegaard, 2020; Lee et al., 2006; Hubler, Wendner and Bazant, 2015).

Accepted manuscript doi:
10.1680/jadcr.24.00078

For early age cement matrix, the autogenous shrinkage δ (Fig. 2a) is the summation of increments of deformation that formed at subsequent time intervals, e.g., δ_{t_n} from t_n to $t_n + \Delta t$. Due to the restraint of one solid particle, the reduction of the shrinkage $\delta_{t_n,r}$ is also made up by an elastic part $\delta_{t_n,r,el}$ and a creep part $\delta_{t_n,r,c}$ (Fig. 2b):

$$\delta_{t_n,r} = \delta_{t_n,r,el} + \delta_{t_n,r,c} = \frac{r}{E_p}\left[(1-\vartheta_p)\sigma_t - \vartheta_p\sigma_r\right]\left(1 + J(t,t_n)E_p(t_n)\right)$$

$$= \frac{p\mathrm{a}^3}{E_p r^2}\left[\frac{1-\vartheta_p}{2}\frac{b^3+2r^3}{b^3-\mathrm{a}^3} + \vartheta_p\frac{b^3-r^3}{b^3-\mathrm{a}^3}\right]\left(1 + J(t,t_n)E_p(t_n)\right) \quad (14)$$

The relationship between the unit linear deformation ε_{t_n} [m/m], i.e., δ_{t_n}/b, and the reduction in the unit linear deformation $\Delta\varepsilon_{t_n}$ [m/m], i.e., $\delta_{t_n,r}/b$, can be expressed:

$$\Delta\varepsilon_{t_n}V = \beta_\theta\varepsilon_{t_n}V_s \quad (15)$$

where

$$\beta_\theta = \frac{3(1-\vartheta_p)}{1+\vartheta_p+2(1-\vartheta_s)(E_p/E_s)/\left(1+J(t,t_n)E_p(t_n)\right)} \quad (16)$$

If the sand/aggregate volume ratio of cement mortar is Φ_A, the relationship between the autogenous shrinkage of cement mortar ε_{m,t_n} and the autogenous shrinkage of corresponding cement paste ε_{p,t_n} during the period from t_n to $t_n + \Delta t$ can be expressed as:

$$\varepsilon_{m,t_n} = \varepsilon_{p,t_n}(1-\Phi_A)^{\beta_\theta} \quad (17)$$

The total autogenous shrinkage of cement mortar $\varepsilon_{m,t_{n+1}}$ is expressed as summation of increments of deformation that formed before time t_{n+1}:

$$\varepsilon_{m,t_{n+1}} = \sum_{i=1}^{n+1}\varepsilon_{m,t_i} = \sum_{i=1}^{n+1}\varepsilon_{p,t_i}(1-\Phi_A)^{\beta_\theta} \quad (18)$$

2. Materials and experiments

3.1 Materials

Portland cement (CEM I 52.5N), Rice husk ash, quartz sand and a polycarboxylate-based water reducer (Glenium 51, BASF) were used in this study. Table 1 shows the chemical composition of Portland cement and rice husk ash (RHA). Mineral composition of Portland cement is given in Table 2. Properties of Portland cement and RHA are shown in Table 3. The specific surface area of Portland cement and RHA in Table 3 was measured by Brunauer-Emmett-Teller nitrogen adsorption/desorption technique. Particle size distribution

of the Portland cement and rice husk ash was measured by Laser Particle Size Analyzer. The measured results are shown in Fig. 3. The mean particle sizes, D50, of Portland cement and RHA are 13.7 μm and 9.0 μm, respectively.

Three types of cement pastes and two types of cement mortars were investigated in this study. Portland cement paste (CEM I 52.5N) served as reference. Two types of RHA cement paste were studied. The RHA dosages in these RHA cement pastes were 10% and 20% by weight of the binder respectively. Portland cement paste and RHA cement paste with 20% rice husk ash were used to prepare mortar mixtures. In both cement mortars, the sand-binder weight ratio was 1. The size of sand used in this study is 0.125 ~ 0.25 mm. Its density is 2650 kg/m^3. The water-binder ratios of all mixtures were 0.25 and the water reducer-binder weight ratio of all mixtures was fixed at 1.6%. Mixture proportion is given in Table 4. A 5L epicyclic Hobart 3.2 Experimental methods

3.2.1 Final setting time

Final setting time of cement pastes and mortars was measured by using Vicat instrument based on standard NEN-EN 196-3:2005 (EN, 2005). The specimen was 40 ± 0.2 millimetres in height. The diameter of the bottom surface of the specimen was 80 ± 1 millimetres, while the diameter of the upper surface of the specimen was 70 ± 1 millimetres. The time when the needle only penetrated 0.5 millimetres into the specimen was the final setting time.

3.2.2 Chemically bound water

Freshly mixed cement paste was casted in a plastic vial. The sample was 5 millimetres in height. Mass of the sample was 5 grams. The sample was stored at 20 °C under sealed condition until testing. At the curing age of 1, 3, and 7 days, the sample was crushed to powder and flushed with liquid nitrogen to cease hydrating. Then the powder was placed in a crucible. The crucible was left overnight in an oven at 105 °C to remove evaporable water and then the mass of the powder was measured. Finally, the powder was placed in a furnace at 950 °C for at least 4 hours. Chemically bound water, which is also called non-evaporable water, was calculated as the change of mass between 105 °C and 950 °C. For each measurement two samples were tested.

3.2.3 Chemical shrinkage

The absolute volume of hydration products is less than the total volume of unhydrated cement and water. This phenomenon is known as chemical shrinkage (Geiker and Knudsen, 1982). About 50 grams of fresh cement paste was placed in an Erlenmeyer flask which was sealed with a rubber stopper. The flask was placed in a water bath. Temperature of the water bath was 20 °C. The capacity of the flask was 250 ml. 1 ml of distilled water was placed above the cement paste and then the flask was filled fully with paraffin oil. A pipette was inserted in the rubber stopper to measure the change of liquid level of the flask. The test lasted seven days. Two samples were measured simultaneously.

3.2.4 Liquid absorption capacity of rice husk ash

One day before testing, rice husk ash was dried in an oven. Temperature of the oven was kept at 105 ˚C. During testing, RHA sample was immersed in water or synthetic pore solution at room temperature. Mass of the RHA sample was 5 grams and volume of the water or synthetic pore solution was 200 ml. Composition of the synthesized pore solution was the same as that used by Jensen (Jensen and Hansen, 2002). The composition of the synthesized pore solution is: $[Na^+]$ = 400 mmol/l, $[K^-]$ = 400 mmol/l, $[Ca^{2+}]$ = 1 mmol/l, $[SO_4^{2-}]$ = 40 mmol/l, $[OH^-]$ = 722 mmol/l. The mixture of RHA and liquid was stirred for 5, 10, 15, 30, and 60 minutes, respectively. In order to remove the liquid sticking to its surface, the wet RHA sample was vacuum filtered with glass fibre filter paper with pore size of 1.6 μm. Then the wet RHA sample was placed in the oven again to get dry RHA sample. Before and after the drying, the RHA sample was weighted. Two samples were tested for each measurement. The absorption capacity C_{ab} of RHA was calculated as:

$$C_{ab} = \frac{m_{wet} - m_{dry}}{m_{dry}} \quad (19)$$

where m_{dry} [g] is the mass of dry RHA sample and m_{wet} [g] is the mass of wet RHA sample.

3.2.5 Water vapour desorption isotherm of rice husk ash

Water vapour desorption isotherm of rice husk ash was determined by using dynamic vapour sorption analyser (TA Q5000 SA). Ten minutes before testing, the RHA sample was submerged in water. Then wet RHA sample weighing 5-10 mg was analysed. The desorption relative humidity point of the water vapour isotherm was set at 98%, 95%, 90%, 80%, 50% and 1%, respectively. Temperature of the sample was kept at 20 ˚C. Two samples were analysed for each test.

3.2.6 Internal relative humidity (RH)

Internal relative humidity of cement pastes was determined by using HC2-AW RH probes. The RH probe was calibrated with saturated salt solution before testing. Error of the measurement was ± 0.5%. Cement paste sample was placed in a container with diameter of 30 millimetres. Thickness of the sample was 7 millimetres. The container was then placed in a temperature-controlled water bath at 20 °C. During the first seven days after mixing, two samples were tested for each measurement. Measured results were recorded every three minutes.

3.2.7 Compressive strength

At the ages of 1, 3, and 7 days, compressive strength of cement pastes and mortars was tested. The samples were cubes with size of 40×40×40 mm^3. Three samples were tested for each measurement.

Accepted manuscript doi:
10.1680/jadcr.24.00078

3.2.8 Autogenous shrinkage

Autogenous deformation of cement pastes and mortars was measured based on ASTM C1698-09 standard (ASTM, 2009) which was proposed by Jensen and Hansen (1995). Freshly mixed cementitious materials were filled into a corrugated tube. The filled tube was then submerged in glycol at 20 ˚C. Liner deformation of the specimen was measured by LVDTs and recorded every five minutes. Length and diameter of the corrugated tube were 440 millimetres and 28.5 millimetres respectively. Measurement accuracy was ±5 μstrain. Three samples were tested simultaneously. Duration of the test was seven days.

3. Experimental results and discussion

4.1 Final setting time

In Fig. 4 the measured final setting time of cement pastes and mortars is shown. It should be noticed that the addition of water reducer causes a delay of final setting time. The final setting time of Portland cement paste with water-cement ratio of 0.3 is around 5 hours (Lu, Li and van Breugel, 2020). In this study, the measured final setting time of Portland cement paste with addition of water reducer (red bar in Fig. 4) is almost 17 hours. Similar phenomenon has also been reported by Van Tuan (2011). Fig. 4 also shows that the final setting time of cement mortar is close to that of corresponding cement paste. Similar results can be found in other literatures (Lu 2019). The effect of addition of quartz sand on final setting time of mixtures is not significant. Final setting time is closely related to the robustness of the microstructure of cementitious materials. Hydration of cement matrix in cement paste or mortar decides the development of the microstructure of the mixture. At the same curing age, the most important influencing factors of the hydration of cement matrix are the type of cement and water-binder ratio (Van Breugel, 1993). The type of cement and water-binder ratio of cement mortar and corresponding cement paste are same. Therefore, the development of microstructure at early age and the final setting time of cement mortar and corresponding cement paste are similar.

From Fig. 4 it can also be found that the final setting time decreases dramatically with increasing RHA dosage. The liquid adsorption capacity of RHA is considerable as shown in Fig. 7. Less free water exists in the RHA cement paste which leads to shorter distance between the unhydrated cement particles. When the water-binder ratio is the same, the microstructure of RHA cement paste is stronger than that of Portland cement paste within the first few hours. Consequently, the final setting time of RHA cement pastes (RHA 0.1 and RHA 0.2), which reflects the stiffness of cementitious material, is shorter than that of Portland cement paste (OPC).

4.2 Chemically bound water

Fig. 5 shows the measured chemically bound water of different cement pastes. From this figure it can be found that the chemically bound water content of RHA cement pastes (RHA 0.1 and RHA 0.2) is higher than that of Portland cement paste (OPC) during the first few

Accepted manuscript doi:
10.1680/jadcr.24.00078

days. But the chemically bound water of Portland cement paste increases faster than that of RHA cement paste. The chemically bound water of cement pastes decreases with the increase of RHA dosage at 7 days. Similar experimental results can be found in other researchers' paper (Zhang, Lastra and Malhotra, 1996.). The higher chemically bound water content of RHA cement paste at early age may owe to the pozzolanic reaction of RHA. Table 1 shows that the amount of SiO_2 in RHA, which will react with calcium hydroxide (CH), is considerable. The chemical reaction between SiO_2 and CH will consume extra water and produce calcium silicate hydrate (Equation 20) (Van Tuan, 2011.). The extra consumed water leads to higher chemically bound water content of RHA cement paste during the first few days. After the first three days, the reaction rate of RHA is very low and the water consumed by the pozzolanic reaction of RHA is few (Huang, 2023). Most of the consumed water is caused by the hydration of Portland cement during this period. Due to the liquid absorption capacity of RHA (as shown in Fig. 7), there is less free water available for Portland cement hydration in RHA cement paste than that in Portland cement paste. Therefore, the chemically bound water content of OPC is higher than that of RHA 0.1 and RHA 0.2 at 7 days.

$$1.1CH + S + 2.8H \rightarrow C_{1.1}SH_{3.9} \quad (20)$$

where CH is the calcium hydroxide; S is silicon dioxide; H is the water and $C_{1.1}SH_{3.9}$ is the calcium silicate hydrate.

4.3 Chemical shrinkage

Chemical shrinkage of Portland cement and RHA cement is shown in Fig. 6. Fig. 6 shows that the chemical shrinkage decreases with increasing dosage of RHA at 7 days. Chemical shrinkage is proportional to the degree of hydration (Parrott et al., 1990). The degree of hydration of Portland cement is about 52% while the reaction degree of RHA is only about 12% at 7 days (Huang, 2023). The addition of RHA will lead to dilution effect, i.e., lower amount of cementitious binder in RHA cement paste (Prasanphan et al., 2010). Less Portland cement in RHA cement paste is available for hydration which results in smaller chemical shrinkage at 7 days.

4.4 Liquid absorption capacity of rice husk ash

Fig. 7 shows the measured liquid absorption capacity of rice husk ash. Horizontal axis in Fig. 7 represents the duration when the RHA sample was immersed in liquid before weighing. From Fig. 7 it can found that liquid is quickly absorbed by RHA particles in first few minutes. The liquid adsorption capacity of RHA is considerable. Weight ratio between absorbed liquid and RHA is around 0.6. There is no change of the weight of absorbed liquid after 10 mins. The considerable liquid adsorption capacity of RHA can be attributed to the capillary action. Based on literature (Van Tuan et al., 2011), there is a porous skeleton in RHA particle and the pore size of RHA particle is smaller than several microns. According to Young-Laplace equation (Equation 21) (Defay et al., 2010), capillary tension will develop when RHA particles are placed in liquid and the liquid will be adsorbed into RHA particles.

$$\sigma_{cap} = -\frac{2\gamma}{r_k} \quad (21)$$

where σ_{cap} [MPa] is the capillary tension; r_k [m] is the Kelvin radius, i.e., the radius of air-liqiud meniscus; γ [N/m] is the surface tension of the liquid.

Fig. 7 also shows that the maximum absorption capacity of rice husk ash in water is larger than that in synthetic pore solution. The ions in solution have a negative effect on the maximum absorption capacity of RHA. As described in Section 2.2.4 the synthetic pore solution used in this study is alkaline solution. Surface tension of the alkaline solution is smaller than that of pure water (Beattie et al., 2010). Smaller surface tension of the alkaline solution results in smaller capillary tension and lower pore solution capacity of RHA (Equation 21).

4.5 Water vapour desorption isotherm of rice husk ash

Fig. 8a shows the measured water vapour desorption isotherm of rice husk ash. From Fig. 8a it can be noticed that the adsorbed water content decreases dramatically, i.e., from 0.61 to 0.06, when RH drops from 100% to 90%. But when RH drops further, i.e., from 80% to 1%, the decrease of adsorbed water content is not significant. This trend is line with the relationship between RH and Kelvin radius. Kelvin radius, which is the radius of air-liquid meniscus, also represents the size of the biggest water-filled pore. Kelvin radius can be calculated based on RH by using Kelvin equation (Equation 22) (von Helmholtz, 1886). Calculated Kelvin radius is shown in Fig. 8b. Fig. 8b shows that the Kelvin radius reduces from 100 nm to 10 nm when RH decreases from 100% to 90%. The pores, ranging from 10nm to 10 μm, are defined as capillary pores (Van Breugel, 1993). The comparison between Fig. 8a and Fig. 8b suggests that most of the absorbed water content is kept in capillary pore. The volume of capillary pore plays a considerable role in the water absorption capacity of RHA.

$$r_k = -\frac{2\gamma V_m}{lnRH_K RT} \quad (22)$$

where V_m [m^3/mol] is the molar volume of the pore solution, its value is taken as 18.02×10^{-6} m^3/mol, i.e., the molar volume of water, in this study; R [J/(mol·K)] is the universal gas constant; T [K] is the absolute temperature; RH_K [-] is RH related to air-liquid menisci.

4.6 Internal relative humidity (RH)

Measured RH of cement pastes is shown in Fig. 9. Drop of the measured relative humidity of cement paste significantly decreases with the increasing dosage of RHA. This phenomenon was also found by other researchers and can be attributed to the internal curing effect of RHA (Rößler, Bui and Ludwig, 2014). Similar to other kinds of internal curing agent, e.g., super-absorbent polymers (SAPs), saturated RHA will release water during the hydration process. RH of Portland cement paste will drop from 98% to 84% during the first 7 days as shown in Fig. 9. About 0.165 grams of water per gram of RHA will release from RHA into the cement paste at this range of relative humidity (Fig. 8). The released water from RHA will

Accepted manuscript doi:
10.1680/jadcr.24.00078

compensate the consumed water relating to self-desiccation and keep the internal relative humidity at a higher level.

4.7 Compressive strength

The measured compressive strength of cement pastes and mortars is displayed in Fig. 10. It can be found that the compressive strength of cement pastes increases with the addition of RHA. Similar results were also reported by other researchers (Van Tuan, 2011; Prasanphan et al., 2010). According to Prasanphan et al. (2010), the higher compressive strength of RHA cement pastes is attributed to two reasons. On one hand, the pozzolanic reaction of RHA results in more production of CSH which plays an important role in compressive strength of cementitious materials (Equation 20). On the other hand, the existence of rice husk ash accelerates the growth of ettringite which is also beneficial for the growth of compressive strength. Apart from the above reasons, liquid absorption capacity of RHA also contributes to the increase of compressive strength. RHA particles added in the mixtures will absorb water and then less free water exists in the RHA cement pastes. The porosity of RHA cement pastes is lower. Lower porosity results in denser skeleton structure and higher compressive strength of RHA cement paste.

From Fig. 10 it can also noticed that the compressive strength of RHA cement mortar is higher than that of Portland cement mortar at the same curing age. Other researchers also found that under certain conditions, e.g., in the case of a mixture with a low water-binder ratio or with the addition of supplementary materials, the strength of mortar or concrete exceeded the strength of corresponding cement paste (Walz, 1970; Scrivener, Bentur and Pratt, 1988). van Breugel (Van Breugel, 1993) points out that the bond between the cement matrix and aggregate will be improved by adding supplementary materials, e.g., silica fume, which leads to higher compressive strength of cement mortar. The chemical composition and pozzolanic properties of RHA are similar to that of silica fume (Table 1). Therefore, the addition of RHA increases the bond strength and then the compressive strength of cement mortar.

4.8 Autogenous shrinkage

Fig. 11 shows the measured results of autogenous shrinkage of different cement pastes and mortars. From Fig. 11 it can be noticed that there are several different stages of measured deformation. After final setting time, the deformations of specimens were measured and recorded. The specimens shrank rapidly during the first few hours. Then there was a brief swelling period after which the specimens shrank again. The difference between the rate of shrinkage before and after the swelling is quite significant. There should be different mechanisms behind different stages. During the hydration process, the absolute volume of hydration products is less than the total volume of unhydrated cement and water. This phenomenon is called chemical shrinkage. Within the first few hours after final setting, the solid skeleton of cement paste is still weak and all the chemical shrinkage turns into external volume reduction. With the progress of hydration, a stronger and stronger solid skeleton forms. Part of chemical shrinkage turns into empty pore inside the cement paste which results

in the formation of water-air meniscus and then autogenous shrinkage. Therefore, it is questionable to take the final setting time as the starting point of autogenous shrinkage (Sant et al., 2006; Chang-Wen et al., 2007). The deformation after the brief swelling period is taken as autogenous shrinkage in this study (Bjøntegaard, 1999; Kovler and Cusson, 2007).

The measured autogenous shrinkage of different mixtures after the brief swelling period is displayed in Fig. 12. The autogenous shrinkage of RHA cement pastes is significantly smaller than that of Portland cement paste. The mitigating effect of RHA on autogenous shrinkage of cement paste is quite pronounced. Fig. 12 also shows that the autogenous shrinkage of cement mortar is dramatically smaller than that of corresponding cement paste. In Section 5.4, the mitigating effect of RHA on autogenous shrinkage and the restraining effect of sand will be discussed in detail.

5. Calculated material parameters and predicted autogenous shrinkage of cement mortar

For the sake of investigating the mitigating effect of rice husk ash on the autogenous shrinkage of cement paste and mortar, internal driving force of autogenous shrinkage and mechanical properties of the materials, i.e., capillary tension and Young's modulus, should be determined first.

5.1 Capillary tension

Autogenous shrinkage is the macroscopic volume reduction related to self-desiccation of cementitious system. While the mechanism of autogenous shrinkage is still under debate, there is general agreement about the existence of a relationship between relative humidity (RH) and autogenous shrinkage (Lura, 2003). Capillary tension is widely accepted as the leading mechanism of autogenous shrinkage in recent years (Kovler and Zhutovsky, 2006). According to Young-Laplace equation (Equation 21), there is a relationship between capillary tension and RH:

$$\sigma_{cap} = -\frac{2\gamma}{r_k} = -\frac{2\gamma}{-\frac{2\gamma V_m}{lnRH_K RT}} = \frac{RTlnRH_K}{V_m} \tag{23}$$

where γ [N/m] is the surface tension of the liquid; r_k [m] is the Kelvin radius, i.e., the radius of air-liqiud meniscus; R [J/(mol·K)] is the universal gas constant; V_m [m^3/mol] is the molar volume of the pore water; T [K] is the absolute temperature; RH_K [-] is the relative humidity related to air-water menisci which can be calculated as:

$$RH_K = \frac{RH_M}{RH_S} \tag{24}$$

where RH_M [-] is the measured relative humidity and RH_S [-] is the effect of dissolved ions on relative humidity.

As shown in Fig. 9, the maximum measured relative humidity of Portland cement paste and RHA cement pastes is lower than 100%. This phenomenon was also found by other researchers (Lura, 2003; Jensen and Hansen, 1996). According to Perrot (1998), the initial

Accepted manuscript doi:
10.1680/jadcr.24.00078

drop of relative humidity is due to the dissolved ions in the pore solution, i.e., RH_S (equation 24). In this study, RH_K of Portland and RHA cement pastes, is calculated by removing the effect of dissolved ions (equation 24) and shown in Fig. 13.

Capillary tension of Portland and RHA cement pastes is calculated by using Equation 23. The calculated results are provided in Fig. 14a. Fig. 14a shows that the capillary tension of Portland cement paste rises from 0 MPa to 22 MPa when RH_K decreases from 100% to 85%. Other researchers also reported similar results (Fig. 14b) (Lebental et al., 2012). From Fig. 14a it can also be noticed that capillary tension decreases with the increase of RHA dosage at 7 days. If more RHA particles are added in the mixtures, more water will be released from RHA into the cement matrix during hydration. The released water leads to the increase of Kelvin radius and then decrease of the capillary tension (equation 23).

5.2 Young's modulus

A lot of empirical equations have been proposed to predict the Young's modulus of cementitious materials during the past few years (ACI, 1992; Gandomi et al., 2015). Young's modulus is calculated as a function of compressive strength in these equations. In this study, the equation proposed by Takafumi et al. (2009) is adopted to predict the Young's modulus of cement paste and mortar:

$$E = k_1 k_2 \varphi {f_c}^{1/3} \rho^2 \quad (25)$$

Where f_c [MPa] is the compressive strength; k_1 [-] is a correction factor which is determined by aggregate; k_1 of cement paste and mortar is 1 and 0.95, respectively (Takafumi et al., 2009); k_2 [-] is a correction factor which is determined by the type of supplementary material. For Portland cement and RHA cement, the value of k_2 is 1 and 1.1, respectively (Takafumi et al., 2009); φ [-] is a fitting coefficient, 1.486×10^{-3} (Takafumi et al., 2009); ρ [Kg/m^3] is the density.

Calculated Young's modulus of different cement pastes and mortars is presented in Fig. 15. The calculated Young's modulus of cement pastes increases with increasing RHA dosage at 7 days. Fig. 15 also shows that Young's modulus of cement mortar is higher than that of corresponding cement paste. The reasons of these phenomena are similar to those of compressive strength which are given in Section 3.7.

5.3 Autogenous shrinkage of mortar

5.3.1 Reference - Portland cement mortar

Measured and predicted autogenous deformations of Mortar OPC are shown in Fig. 16. The predicted autogenous shrinking of Mortar OPC is obtained by using Equation 18 based on the measured autogenous shrinking of corresponding cement paste (red line in Fig. 16). Fig. 16 shows that the autogenous shrinkage of Mortar OPC is markedly reduced by adding quartz sand (quartz sand-binder weight ratio is 1). The restraining effect of sand on autogenous

shrinkage is pronounced. Prediction of the autogenous shrinkage of Mortar OPC with improved Pickett model (blue line) is better than that with Pickett model (green line). It illustrates that visco-elastic behaviour of cement paste plays an important role in the restraining effect of sand on the autogenous shrinkage. Accuracy of the predictions is improved by taking creep into account.

5.3.2 Portland cement mortar with addition of 20% RHA

Fig. 17 shows the measured and predicted autogenous deformations of Mortar RHA 0.2. The RHA-binder weight ratio and sand-binder weight ratio of Mortar RHA 0.2 are 0.2 and 1. It can be found that the autogenous shrinkage of Mortar RHA 0.2 at 7 days is much smaller than that of Mortar OPC. The influence of rice husk ash on the autogenous shrinkage of cement mortar is quite significant. Similar to the results of Mortar OPC, prediction of autogenous shrinkage of Mortar RHA 0.2 is also improved by taking creep into consideration. Visco-elastic behaviour of cement matrix is also very important for the autogenous shrinkage of RHA cement mortar.

5.4 Discussion

In this study, the influence of rice husk ash on the autogenous shrinkage of cementitious materials was investigated. The measured deformations of Portland cement paste with and without addition of RHA were shown in Fig. 12. The measurement results showed that the mitigating effect of RHA on the autogenous shrinkage increased with the increasing dosage of RHA. When the dosage of RHA increased from 0% to 20%, the autogenous shrinkage of cement paste decreased from 600 μstrain to 65 μstrain at 7 days. The mitigating effect of rice husk ash on the autogenous shrinkage of cement paste may mainly be attributed to two factors. Firstly, due to the internal curing effect of RHA, the self-desiccation of the hydrating cement paste was mitigated. During the hydration process, free water was consumed and internal relative humidity (RH) of cement paste dropped. For the RHA cement paste, the water adsorbed on the RHA particles released into cement paste (Fig. 8) and kept RH at higher level (Fig. 9). It is widely accepted that capillary tension, which is a function of RH, is the leading mechanism of autogenous shrinkage. Higher RH resulted in smaller capillary tension (Fig. 14). Secondly, the mechanical properties of cement paste were improved by adding RHA. At the same age, compressive strength (Fig. 10) and Young's modulus of RHA cement pastes (Fig. 15) were larger than those of Portland cement paste. The stiffness of RHA cement pastes was higher than that of Portland cement paste. Stiffness reflects the resistance of material to deformation. With the same internal driving force, cement paste with higher stiffness exhibits smaller autogenous shrinkage. Both the two mentioned factors contribute to smaller autogenous shrinkage of RHA cement pastes.

It should also be noted that the measured autogenous deformation of cement pastes was the consequence of two competitive processes which are an expansion process and a shrinkage process. After the brief swelling period (Fig. 11), the shrinkage process was predominant but the expansion mechanism still existed and influenced the development of the autogenous

shrinkage. The released water from RHA may also affect the expansion mechanism, e.g., crystallization pressure (Steiger, 2005), and result in bigger early-age expansion. Bigger early-age expansion also contributes to smaller measured autogenous shrinkage of RHA cement paste. More attention should be given to the influence of RHA on the expansion mechanisms in further research.

Autogenous shrinkage of Portland cement mortars with and without addition of rice husk ash was experimentally studied. The measured results showed that the autogenous shrinkage of cement mortar was much smaller than that of corresponding cement paste (Fig. 12). One reason of this phenomenon is the 'diluting effect' of sand. Cement mortar is mainly made up by two phases, i.e., sand particles and the cement matrix. The autogenous shrinkage only occurs in the cement matrix. A considerable part of cement mortar is the non-shrinking sand. Therefore, unit autogenous shrinkage of cement mortar was smaller than that of corresponding cement paste. The other reason is the restraining effect of quartz sand on the autogenous shrinkage of surrounding cement matrix. Due to the restraint of quartz sand, the shrinkage of the cement matrix was reduced (Fig. 2). Both these two reasons led to smaller autogenous shrinkage of cement mortars. Fig. 12 also showed that the combining effect of RHA and quartz sand on the mitigation of autogenous shrinkage was quite pronounced. The autogenous shrinkage of Mortar RHA 0.2 was only 65 μstrain at 7 days. Due to the fact that the mechanical properties of RHA cement mortar were also better than that of Portland cement mortar, the cracking potential of RHA cement mortar related to the autogenous shrinkage was much lower than that of Portland cement mortar. Therefore, rice husk ash is a promising internal curing agent which can be used to mitigate the autogenous shrinkage and reduce the cracking potential of UHPC, which is made of large volume of aggregate contents.

Comparisons between the measured and predicted results showed that the autogenous shrinkage of cement mortars could be predicted more accurately by using improved Pickett model (Fig. 16 and Fig. 17). In Pickett model, both quartz sand and the cement matrix were taken as elastic materials. But cement matrix is not an ideal elastic material. Ignorance of the visco-elastic behaviour of the cement matrix, i.e., creep, would result in overestimation of the autogenous shrinkage of cement mortars (Fig. 16 and Fig. 17). In the improved Pickett model, the visco-elastic behaviour of the cementitious materials was taken into account. The discrepancies between the measured autogenous shrinkage of cement mortars and the calculated results with improved Pickett model were small. But it should be kept in mind that there was still difference between the measured and calculated autogenous shrinkage (Fig. 16 and Fig. 17), 30 μstrain for Portland cement mortar and 3 μstrain for RHA cement mortar at seven days. The difference may attribute to other reasons which haven't been taken into account in the proposed model, e.g., micro-cracking (Wei, 2008).

6 Further discussions

As mention in section 4.8, there is still no consensus about the starting point of autogenous shrinkage. The Japan Concrete Institute (JCI) (Tazawa, 1999) takes the deformation after initial setting time as autogenous shrinkage, whereas the final setting time is considered as

Accepted manuscript doi:
10.1680/jadcr.24.00078

the beginning of autogenous shrinkage in the American Standard Test Method (ASTM) (ASTM, 2009). According to Bjøntegaard and Kovler (Bjøntegaard, 1999; Kovler and Cusson, 2007), the time when the maximum (macroscopically) swelling is observed can be taken as the starting time of autogenous shrinkage. Beside these opinions, meniscus depression measurement, i.e., change of relative humidity (Equation 23), is also used to determine the starting point of autogenous shrinkage (Chang-Wen et al., 2007; Huang and Ye, 2017). In this section, the onset of measured relative humidity drop (Figure 9) is taken as the 'time-zero' of autogenous shrinkage. The measured autogenous shrinkage of different cement pastes and mortars after 'time-zero' is shown in Figure 18 (Chang-Wen et al., 2007). Autogenous shrinkage of cement mortars after 'time-zero' is also simulated by using the Pickett model and improved Pickett model (Figure 19 (Chang-Wen et al., 2007)). Comparisons between the measured and predicted results showed that the autogenous shrinkage of cement mortars after 'time-zero' could still be predicted quite well by using improved Pickett model.

7 Conclusions

In this study, autogenous shrinkage of cement mortars with and without addition of rice husk ash (RHA) was experimentally and numerically studied. A numerical model, i.e., improved Pickett model, was adopted to predict the autogenous shrinkage of Portland cement mortar and rice husk ash blended cement mortar. In this model, the visco-elastic behaviour of the cementitious materials, i.e., creep, was taken into consideration. Comparisons between the measured and predicted results showed that the autogenous shrinkage of cement mortars could be predicted more accurately by taking the creep into consideration. Creep plays a big part in the autogenous shrinkage of both Portland cement mortar and rice husk ash blended cement mortar and must not be ignored. But it should still be kept in mind that there was still difference between the measured and calculated autogenous shrinkage, 30 μstrain for Portland cement mortar and 3 μstrain for RHA cement mortar at seven days. The difference may attribute to other reasons which haven't been taken into account in the proposed model, e.g., micro-cracking.

Liquid absorption capacity and water vapour desorption isotherm of RHA were also tested. Influence of RHA on the material properties of Portland cement paste was also investigated experimentally. According to the measurement results, the liquid absorption capacity of RHA was considerable. A large amount of adsorbed water released from RHA to the cement matrix during hydration. At 7 days, compressive strength of RHA cement paste was higher than that of Portland cement paste. Due to the extra supplementary water, drop of RH of cement pastes significantly decreased with the addition of RHA. The measured results showed that both chemical shrinkage and autogenous shrinkage decreased with the addition of RHA. The mitigating effect of rice husk ash on the autogenous shrinkage of cement paste and mortar was pronounced. Due to the fact that the mechanical properties of RHA cement mortar were also better than that of Portland cement mortar, RHA is a promising internal curing agent

which can be used to mitigate the autogenous shrinkage and reduce the cracking potential of UHPC.

Data Availability Statement

Some or all data, models, or code that support the findings of this study are available from the corresponding author upon reasonable request.

Acknowledgment

The authors would like to acknowledge the funding supported by the National Natural Science Foundation of China (Grant Nos. 42271146) and the China Scholarship Council (CSC).

CRediT authorship contribution statement

Tianshi Lu: Writing - original draft, Methodology, Software, Conceptualization. Han Yang: Software, Writing - review & editing. Hao Huang: Conceptualization, Methodology. Xiang Zhao: Software.

Notations

σ_t	normal stress perpendicular to the radius	[MPa]
p	unit pressure between inner solid particle and outer cement matrix	[MPa]
r	radial coordinate	[m]
a	radius of inner solid particle	[m]
b	radius of cement matrix shell	[m]
σ_r	normal stress in the radial direction	[MPa]
ε	unit linear deformation	[m/m]
V	volume of the cement matrix	[m^3]
ϑ_p	Poisson ratio of the cement matrix	[-]

E_p	Young's modulus of the cement matrix	[MPa]
V_s	volume of inner solid particle	[m^3]
$\Delta\varepsilon$	reduction in the unit linear deformation	[m/m]
ϑ_s	Poisson ratio of inner solid particle	[-]
E_s	Young's modulus of inner solid particle	[MPa]
Φ_A	sand/aggregate volume ratio of cement mortar	[-]
ε_m	shrinkage of cement mortar	[m/m]
ε_p	shrinkage of corresponding cement paste	[m/m]
t	time	[days]
$\varepsilon_e(t)$	elastic deformation at time t	[m/m]
$\varepsilon_c(t)$	creep at time t	[m/m]
$\sigma(t)$	applied stress of cement matrix at time t	[MPa]
t_0	time when the load is applied	[days]
$J(t,t_0)$	creep compliance	[MPa^{-1}]
E_i	instantaneous modulus	[MPa]
P_1	viscoelastic compliance	[MPa^{-1}]
β	time constant	[days]
P_2	flow constant	[MPa^{-1}]
K	rate constant	[$days^{-1}$]
m_{dry}	mass of dry RHA sample	[g]
m_{wet}	mass of wet RHA sample	[g]
σ_{cap}	capillary tension	[MPa]
r_k	Kelvin radius	[m]
γ	surface tension of the liquid	[N/m]
V_m	molar volume of the pore solution	[m^3/mol]
R	universal gas constant	[J/(mol·K)]
T	absolute temperature	[K]

RH_K	RH related to air-liquid menisci	[-]
RH_M	measured relative humidity	[-]
RH_S	effect of dissolved ions on relative humidity	[-]
f_c	compressive strength	[MPa]
k_1	correction factor which is determined by aggregate	[-]
k_2	correction factor which is determined by the type of supplementary material	[-]
φ	fitting coefficient	[-]
ρ	density	[Kg/m^3]

References

American Concrete Institute (ACI), 1992. State-of-the-art report on high-strength concrete. American Concrete Institute, Farmington Hills, Michigan.

Amin, M.N., Hissan, S., Shahzada, K., Khan, K. and Bibi, T., 2019. Pozzolanic reactivity and the influence of rice husk ash on early-age autogenous shrinkage of concrete. Frontiers in Materials, 6, p.150.

ASTM, A., 2009. C1698-09 Standard test method for autogenous strain of cement paste and mortar. ASTM International, West Conshohocken, PA.

Bažant, Z.P. and Osman, E., 1976. Double power law for basic creep of concrete. Matériaux et Construction, 9, pp.3-11.

Bažant, Z.P. and Chern, J.C., 1985. Triple power law for concrete creep. Journal of Engineering Mechanics, 111(1), pp.63-83.

Bazant, Z.P. and Prasannan, S., 1989a. Solidification theory for concrete creep. I: Formulation. Journal of engineering mechanics, 115(8), pp.1691-1703.

Bažant, Z.P. and Prasannan, S., 1989b. Solidification theory for concrete creep. II: Verification and application. Journal of Engineering mechanics, 115(8), pp.1704-1725.

Beattie, J.K., Djerdjev, A.M., Gray-Weale, A., Kallay, N., Lützenkirchen, J., Preočanin, T. and Selmani, A., 2014. pH and the surface tension of water. Journal of colloid and interface science, 422, pp.54-57.

Bentz, D.P. and Jensen, O.M., 2004. Mitigation strategies for autogenous shrinkage cracking. Cement and Concrete Composites, 26(6), pp.677-685.

Bentz, D.P. and Weiss, W.J., 2011. Internal curing: a 2010 state-of-the-art review (pp. 1-82). Gaithersburg: US Department of Commerce, National Institute of Standards and Technology.

Bjøntegaard, Ø., 1999. Thermal dilation and autogenous deformation as driving forces to self-induced stresses in high performance concrete. Norges Teknisk-Naturvitenskapelige Universitet.

Boateng, A.A. and Skeete, D.A., 1990. Incineration of rice hull for use as a cementitious material: The Guyana experience. Cement and Concrete Research, 20(5), pp.795-802.

Van Breugel, K., 1980. Relaxation of young concrete, Report. Delft University of Technology, 144.

Van Breugel, K., 1993. Simulation of hydration and formation of structure in hardening cement-based materials. Delft University of Technology.

Chandrasekhar, S.A.T.H.Y., Satyanarayana, K.G., Pramada, P.N., Raghavan, P. and Gupta, T.N., 2003. Review processing, properties and applications of reactive silica from rice husk—an overview. Journal of materials science, 38, pp.3159-3168.

Chang-Wen, M., Qian, T., Wei, S. and Jia-Ping, L., 2007. Water consumption of the early-age paste and the determination of "time-zero" of self-desiccation shrinkage. Cement and concrete research, 37(11), pp.1496-1501.

CT, A., 13, ACI Concrete Terminology, American Concrete Institute, Farmington Hills, MI, 2013.

Della, V.P., Kühn, I. and Hotza, D., 2002. Rice husk ash as an alternate source for active silica production. Materials letters, 57(4), pp.818-821.

Delsaute, B., Torrenti, J.M. and Staquet, S., 2017. Modeling basic creep of concrete since setting time. cement and concrete composites, 83, pp.239-250.

Defay, R., Prigogine, I., Bellemans, A. and Everett, D.H., 1966. Surface tension and adsorption.

EN, T., 2005. 196-3, Methods of testing cement-part 3: determination of setting time and soundness. BSI Group, London, UK.

Fehling, E., Schmidt, M., Walraven, J., Leutbecher, T. and Fröhlich, S., 2014. Ultra-high performance concrete UHPC. Ernst & Sohn: Berlin, Germany, pp.25-32.

Gandomi, A.H., Faramarzifar, A., Rezaee, P.G., Asghari, A. and Talatahari, S., 2015. New design equations for elastic modulus of concrete using multi expression programming. Journal of Civil Engineering and Management, 21(6), pp.761-774.

Geiker, M. and Knudsen, T., 1982. Chemical shrinkage of Portland cement pastes. Cement and Concrete Research, 12(5), pp.603-610.

Geiker, M.R., Bentz, D.P. and Jensen, O.M., 2004. Mitigating autogenous shrinkage by internal curing. ACI Special Publications, pp.143-154.

Gifta, C.C., Prabavathy, S. and Kumar, G.Y., 2013. Study on internal curing of high performance concrete using super absorbent polymers and light weight aggregates.

Grasley, Z.C., Lange, D.A., Brinks, A.J. and D'Ambrosia, M.D., 2005. Modeling autogenous shrinkage of concrete accounting for creep caused by aggregate restraint. In Proceedings of the 4th international seminar on self-desiccation and its importance in concrete technology, NIST, Gaithersburg, MD (pp. 78-94).

Grasley, Z.C., 2006. Measuring and modeling the time-dependent response of cementitious materials to internal stresses (Doctoral dissertation, University of Illinois at Urbana-Champaign).

Hammer, T.A. and Sellevold, E.J., 2004. Internal curing role of absorbed water in aggregates. Special Publication, 218, pp.131-142.

Hansen, T.C. and Nielsen, K.E., 1965, July. Influence of aggregate properties on concrete shrinkage. In Journal Proceedings (Vol. 62, No. 7, pp. 783-794).

Hedegaard, B., 2020. Creep and shrinkage modeling of concrete using solidification theory. Journal of Materials in Civil Engineering, 32(7), p.04020179.

von Helmholtz, R., 1886. Untersuchungen über Dämpfe und Nebel, besonders über solche von Lösungen. Annalen der Physik, 263(4), pp.508-543.

Hobbs, D.W., 1974, September. Influence of aggregate restraint on the shrinkage of concrete. In Journal Proceedings (Vol. 71, No. 9, pp. 445-450).

Holt, E.E., 2001. Early age autogenous shrinkage of concrete. University of Washington.

Holt, E., 2002, June. Very early age autogenous shrinkage: governed by chemical shrinkage or self-desiccation. In Proceedings of the Third International Research Seminar in Lund, Lund, Sweden (pp. 1-25).

Huang, H. and Ye, G., 2017. Examining the "time-zero" of autogenous shrinkage in high/ultra-high performance cement pastes. Cement and Concrete Research, 97, pp.107-114.

Huang, H., 2023. Mitigating the autogenous shrinkage of ultra-high performance concrete by using rice husk ash. Delft University of Technology.

Hubler, M.H., Wendner, R. and Bazant, Z.P., 2015. Comprehensive database for concrete creep and shrinkage: analysis and recommendations for testing and recording. ACI Materials Journal, 112(4), p.547.

Jensen, M. and Hansen, P.F., 1996. Autog enous deformation and change of the relative humidity in silica fume-modified cement paste. Materials Journal, 93(6), pp.539-543.

Jensen, O.M. and Hansen, P.F., 2001. Water-entrained cement-based materials: I. Principles and theoretical background. Cement and concrete research, 31(4), pp.647-654.

Jensen, O.M. and Hansen, P.F., 2002. Water-entrained cement-based materials: II. Experimental observations. Cement and concrete research, 32(6), pp.973-978.

Jiang, N., Ge, Z., Wang, Z., Gao, T., Zhang, H., Ling, Y. and Šavija, B., 2024. Size effect on compressive strength of foamed concrete: Experimental and numerical studies. Materials & Design, 240, p.112841.

Justs, J., Wyrzykowski, M., Bajare, D. and Lura, P., 2015. Internal curing by superabsorbent polymers in ultra-high performance concrete. Cement and concrete research, 76, pp.82-90.

Kang, S.H., Hong, S.G. and Moon, J., 2019. The use of rice husk ash as reactive filler in ultra-high performance concrete. Cement and Concrete Research, 115, pp.389-400.

Klug, P. and Wittmann, F., 1974. Activation energy and activation volume of creep of hardened cement paste. Materials science and Engineering, 15(1), pp.63-66.

Kovler, K. and Zhutovsky, S., 2006. Overview and future trends of shrinkage research. Materials and structures, 39, pp.827-847.

Kovler, K. and Cusson, D., 2007. Effects of internal curing on autogenous deformation. Internal Curing of Concrete-State-of-the-Art Report of RILEM Technical Committee, 196, pp.71-104.

Lebental, B., Moujahid, W., Lee, C.S., Maurice, J.L. and Cojocaru, C.S., 2012, May. Graphene-based resistive humidity sensor for in-situ monitoring of drying shrinkage and intrinsic permeability in concrete. In NICOM 4: 4th International Symposium on Nanotechnology in Construction (p. 8p).

Lee, Y., Yi, S.T., Kim, M.S. and Kim, J.K., 2006. Evaluation of a basic creep model with respect to autogenous shrinkage. Cement and concrete research, 36(7), pp.1268-1278.

Li, Z., Lu, T., Chen, Y., Wu, B. and Ye, G., 2021. Prediction of the autogenous shrinkage and microcracking of alkali-activated slag and fly ash concrete. Cement and Concrete Composites, 117, p.103913.

Li, C., Jiang, D., Li, X., Lv, Y. and Wu, K., 2023. Autogenous shrinkage and hydration property of cement pastes containing rice husk ash. Case Studies in Construction Materials, 18, p.e01943.

Lu, T., 2019. Autogenous shrinkage of early age cement paste and mortar. Delft University of Technology.

Lu, T., Li, Z. and van Breugel, K., 2020. Modelling of autogenous shrinkage of hardening cement paste. Construction and Building Materials, 264, p.120708.

Lu, T., Liang, X., Liu, C., Chen, Y. and Li, Z., 2023. Experimental and numerical study on the mitigation of autogenous shrinkage of cementitious material. Cement and Concrete Composites, 141, p.105147.

Lura, P., Jensen, O.M. and Van Breugel, K., 2003. Autogenous shrinkage in high-performance cement paste: An evaluation of basic mechanisms. Cement and concrete research, 33(2), pp.223-232.

Lura, P., 2003. Autogenous deformation and internal curing of concrete. Technische Universiteit Delft.

Mabrouk, R., Ishida, T. and Maekawa, K., 2004. A unified solidification model of hardening concrete composite for predicting the young age behavior of concrete. Cement and Concrete Composites, 26(5), pp.453-461.

Mechtcherine, V., Dudziak, L. and Hempel, S., 2009. Internal curing to reduce cracking potential of ultra high performance concrete by means of super absorbent polymers. In Proceedings of 2nd International RILEM Workshop on Concrete Durability and Service Life Planning (ConcreteLife09) (Vol. 10).

Meddah, M.S., Suzuki, M. and Sato, R., 2011. Influence of a combination of expansive and shrinkage-reducing admixture on autogenous deformation and self-stress of silica fume high-performance concrete. Construction and Building Materials, 25(1), pp.239-250.

Mejlhede Jensen, O. and Freiesleben Hansen, P., 1995. A dilatometer for measuring autogenous deformation in hardening Portland cement paste. Materials and structures, 28, pp.406-409.

Noguchi, T., Tomosawa, F., Nemati, K.M., Chiaia, B.M. and Fantilli, A.P., 2009. A practical equation for elastic modulus of concrete. ACI Structural Journal, 106(5), p.690.

Parrott, L.J., Geiker, M., Gutteridge, W.A. and Killoh, D., 1990. Monitoring Portland cement hydration: comparison of methods. Cement and concrete research, 20(6), pp.919-926.

Perrot, P., 1998. A to Z of Thermodynamics. Oxford University Press, USA.

Persson, B., 1997. Self-desiccation and its importance in concrete technology. Materials and Structures, 30, pp.293-305.

Pickett, G., 1956, January. Effect of aggregate on shrinkage of concrete and a hypothesis concerning shrinkage. In Journal Proceedings (Vol. 52, No. 1, pp. 581-590).

Prasanphan, S., Sanguanpak, S., Wansom, S. and Panyathanmaporn, T., 2010. Effects of ash content and curing time on compressive strength of cement paste with rice husk ash. Suranaee Journal of Science and Technology, 17(3), pp.293-302.

Rößler, C., Bui, D.D. and Ludwig, H.M., 2014. Rice husk ash as both pozzolanic admixture and internal curing agent in ultra-high performance concrete. Cement and Concrete Composites, 53, pp.270-278.

Sant, G., Rajabipour, F., Lura, P. and Weiss, J., 2006. Examining time-zero and early age expansion in pastes containing shrinkage reducing admixtures (SRA's). In Proc., 2nd RILEM Symp. on Advances in Concrete through Science and Engineering.

SAP, R.T., 2012. Application of Superabsorbent Polymers (SAP) in Concrete Construction. RILEM State-of-the-Art Report Prepared by Technical Committee, 165.

Schmidt, M. and Fehling, E., 2005. Ultra-high-performance concrete: research, development and application in Europe. ACI Spec. Publ, 228(1), pp.51-78.

Scrivener, K.L., Bentur, A. and Pratt, P.L., 1988. Quantitative characterization of the transition zone in high strength concretes. Advances in Cement Research, 1(4), pp.230-237.

de Sensale, G.R., Ribeiro, A.B. and Gonçalves, A., 2008. Effects of RHA on autogenous shrinkage of Portland cement pastes. Cement and Concrete Composites, 30(10), pp.892-897.

Shen, P., Lu, L., He, Y., Rao, M., Fu, Z., Wang, F. and Hu, S., 2018. Experimental investigation on the autogenous shrinkage of steam cured ultra-high performance concrete. Construction and building materials, 162, pp.512-522.

Steiger, M., 2005. Crystal growth in porous materials—I: The crystallization pressure of large crystals. Journal of crystal growth, 282(3-4), pp.455-469.

Tawfek, A.M., Ge, Z., Yuan, H., Zhang, N., Zhang, H., Ling, Y., Guan, Y. and Šavija, B., 2023. Influence of fiber orientation on the mechanical responses of engineering

cementitious composite (ECC) under various loading conditions. Journal of Building Engineering, 63, p.105518.

Tazawa, E.I., 1999. Autogenous shrinkage of concrete. CRC Press.

Timoshenko, S , and Goodier, J. N., 1951. Theory Of Elasticity. 2nd Ed. McGraw-Hill.

Van Tuan, N., Ye, G. and van Breugel, K., 2010, August. Effect of rice husk ash on autogenous shrinkage of ultra high performance concrete. In Proceedings of the International RILEM Conference on Advances in Construction Materials through Science and Engineering, Hong Kong, China (pp. 4-7).

Van Tuan, N., Ye, G., Van Breugel, K., Fraaij, A.L. and Dai Bui, D., 2011. The study of using rice husk ash to produce ultra high performance concrete. Construction and Building Materials, 25(4), pp.2030-2035.

Van Tuan, N., 2011. Rice husk ash as a mineral admixture for ultra high performance concrete. Technische Universiteit Delft.

Vieira, A.P., Toledo Filho, R.D., Tavares, L.M. and Cordeiro, G.C., 2020. Effect of particle size, porous structure and content of rice husk ash on the hydration process and compressive strength evolution of concrete. Construction and Building Materials, 236, p.117553.

Vieira, A.P., Toledo Filho, R.D., Tavares, L.M. and Cordeiro, G.C., 2022. Mitigation of autogenous shrinkage of high-strength concrete using rice husk ashes with distinct pore structures. Advances in Cement Research, 34(4), pp.151-160.

Walz, K., 1970. Beziehung zwischen Wasserzementwert, Normfestigkeit des Zements (DIN 1164, Juni 1970) und Betondruckfestigkeit. beton, 20(11), pp.499-503.

Wang, Y., Xia, A., Zhang, P. and Qin, G., 2022. Probabilistic physical modeling of randomly corroded surface and its use in reliability analysis of corroded pipelines under spatiotemporal vibration. Ocean Engineering, 262, p.112219.

Wei, Y., 2008. Modeling of autogenous deformation in cementitious materials, restraining effect from aggregate, and moisture warping in slabs on grade. University of Michigan.

Wyrzykowski, M., Lura, P., Pesavento, F. and Gawin, D., 2011. Modeling of internal curing in maturing mortar. Cement and Concrete Research, 41(12), pp.1349-1356.

Yang, L., Shi, C. and Wu, Z., 2019. Mitigation techniques for autogenous shrinkage of ultra-high-performance concrete–A review. Composites Part B: Engineering, 178, p.107456.

Zhang, M.H., Lastra, R. and Malhotra, V.M., 1996. Rice-husk ash paste and concrete: some aspects of hydration and the microstructure of the interfacial zone between the aggregate and paste. Cement and concrete Research, 26(6), pp.963-977.

Zhang, X., Liu, Z. and Wang, F., 2019. Autogenous shrinkage behavior of ultra-high performance concrete. Construction and Building Materials, 226, pp.459-468.

Zhu, T.Y., 2012. Some useful numbers on the engineering properties of Materials (geologic and otherwise), GEOL 615, Department of Geophysics.

Tables

Table 1. Chemical composition of Portland cement and rice husk ash (% by weight)

Chemical Composition	CEM I 52.5N	RHA
SiO_2	24.0	88.9
Al_2O_3	5.0	0.3
CaO	64.0	1.7
Fe_2O_3	3.0	0.2
K_2O	-	4.2
SO_3	2.4	0.6
Na_2O	0.3	-
Total	98.7	95.9

Table 2. Mineral composition of Portland cement (% by weight)

Phase	Weight (%)
C_3S	63.77
C_2S	9.24
C_3A	8.18
C_4AF	9.13
Other	9.68

Table 3. Properties of Portland cement and rice husk ash

Properties	CEM I 52.5N	RHA
Specific gravity (g/cm^3)	3.15	2.10
Specific surface area (m^2/g)	1.29	29.70
Loss on ignition (LOI)	1.30	2.51

Accepted manuscript doi:
10.1680/jadcr.24.00078

Table 4. Mixture proportion of cement pastes and mortars (% by weight)

Sample	CEM I 52.5N (%)	Sand (%)	RHA (%)	Water reducer-binder ratio (%)	Water-binder ratio (w/b)
OPC	100	0	0	1.6	0.25
RHA 0.1	90	0	10	1.6	0.25
RHA 0.2	80	0	20	1.6	0.25
Mortar OPC	50	50	0	1.6	0.25
Mortar RHA 0.2	40	50	10	1.6	0.25

Figure captions

Fig. 1. The normal stress perpendicular to the radius σ_t and the normal stress in the radial direction σ_r.

Fig. 2. Schematic diagram of the restraint of inner solid particle.

Fig. 3. Particle size distribution of the Portland cement and rice husk ash.

Fig. 4. Experimental results of final setting time.

Fig. 5. Measured results of chemically bound water.

Fig. 6. Measured results of chemical shrinkage.

Fig. 7. Measured absorption capacity of RHA.

Fig. 8. Measured water vapour desorption isotherm of RHA and calculated Kelvin radius as a function of RH.

Fig. 9. Measured results of internal relative humidity.

Fig. 10. Measured results of compressive strength.

Fig. 11. Measured results of autogenous shrinkage after final setting time.

Fig. 12. Measured results of autogenous shrinkage after the brief swelling period.

Fig. 13. Relative humidity related to air-liquid menisci RH_K of Portland and RHA cement pastes.

Fig. 14. Calculated capillary tension of different mixtures and capillary tension reported by Lebental et al. (2012).

Fig. 15. Calculated results of Young's modulus.

Fig. 16. Measured and predicted results of autogenous shrinkage of Mortar OPC after the brief swelling period.

Fig. 17. Measured and predicted results of autogenous shrinkage of Mortar RHA 0.2 after the brief swelling period.

Accepted manuscript doi:
10.1680/jadcr.24.00078

Fig. 18. Measured results of autogenous shrinkage after the onset of relative humidity drop (Chang-Wen et al., 2007).

Fig. 19. Measured and predicted results of autogenous shrinkage of cement mortars after the onset of relative humidity drop (Chang-Wen et al., 2007).

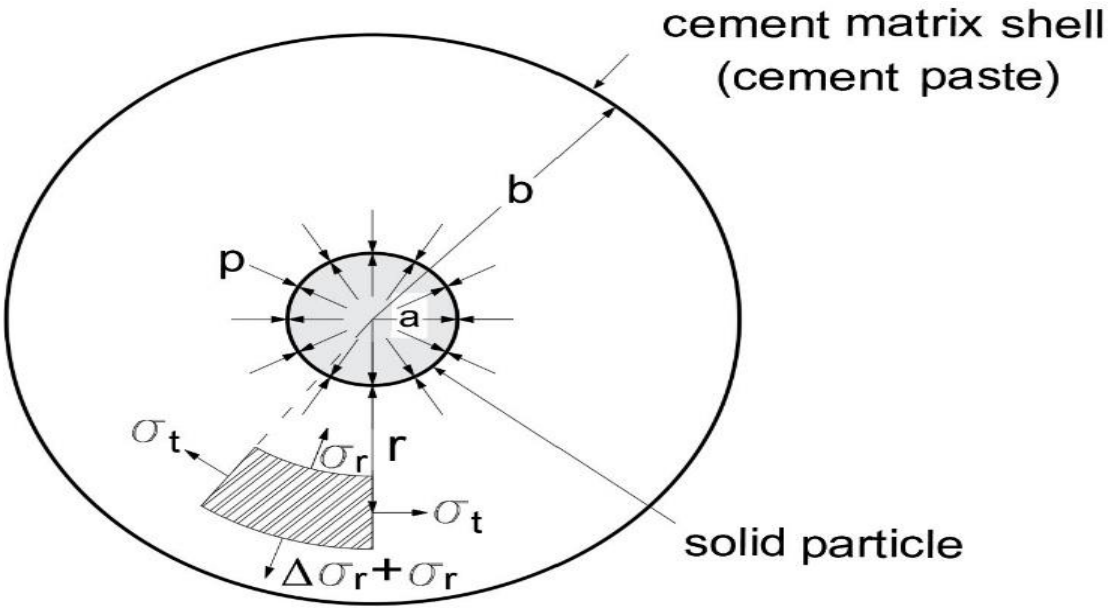

Figure 1

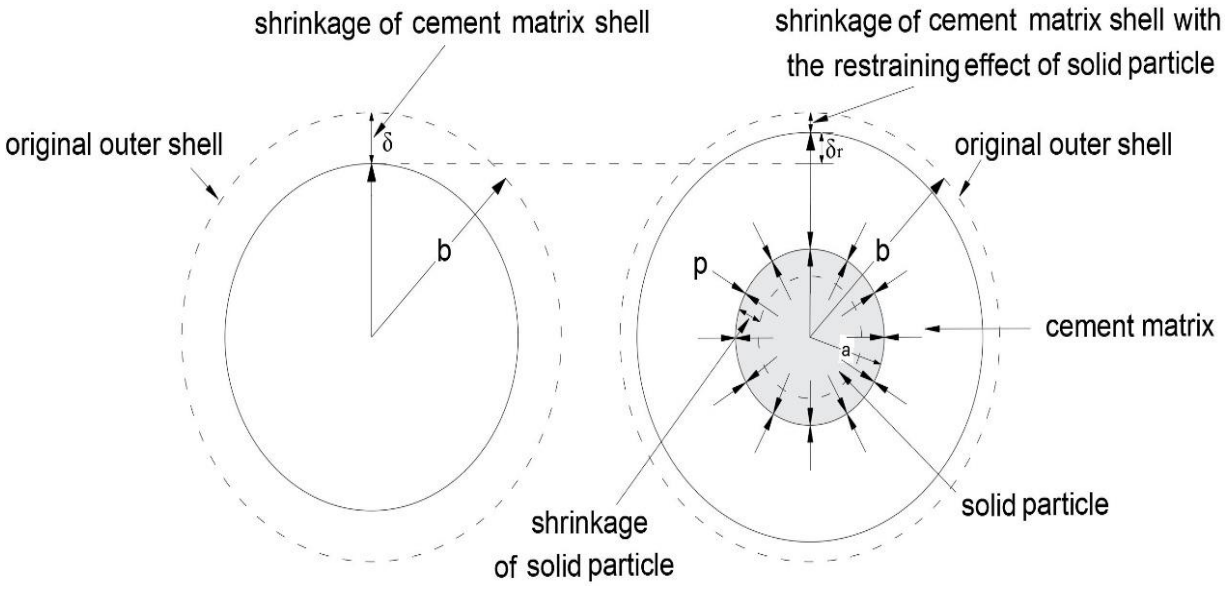

Accepted manuscript doi:
10.1680/jadcr.24.00078

Figure 2

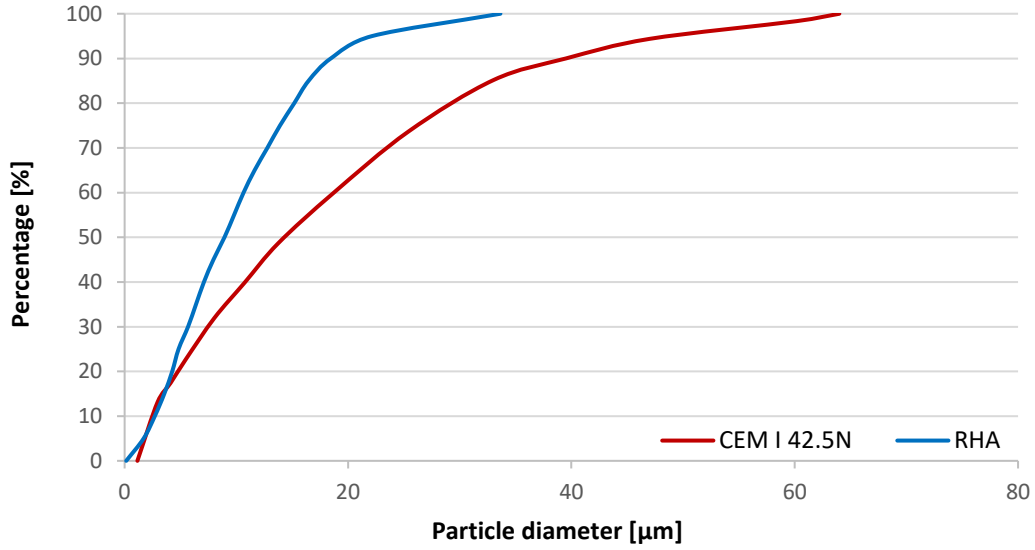

Figure 3

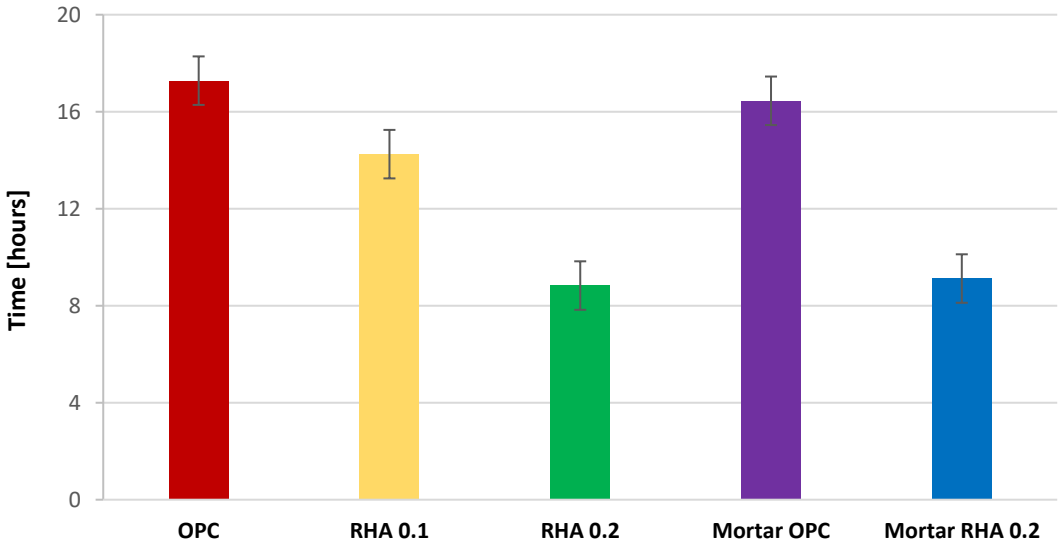

Figure 4

Accepted manuscript doi:
10.1680/jadcr.24.00078

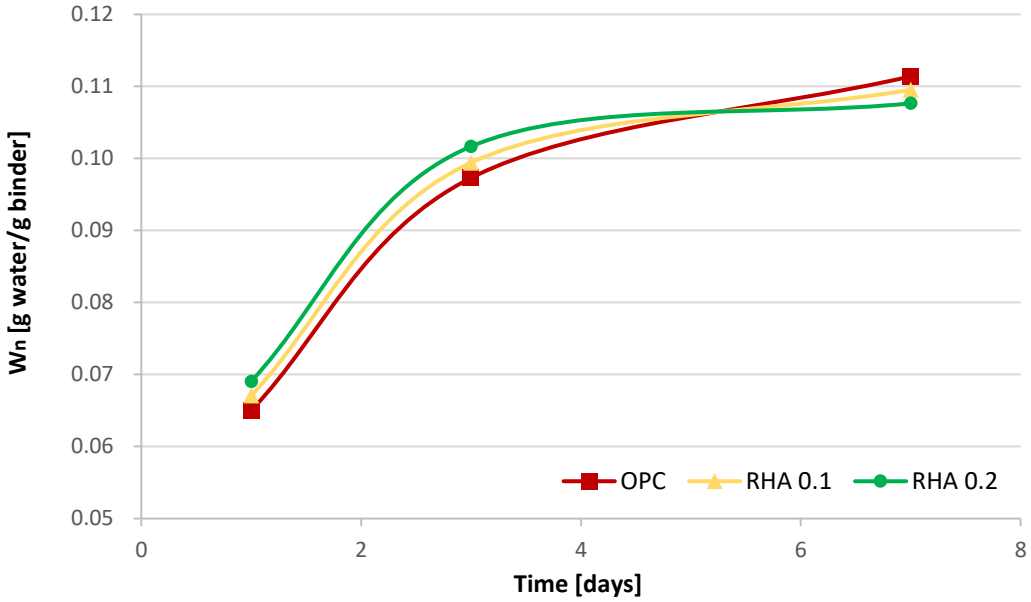

Figure 5

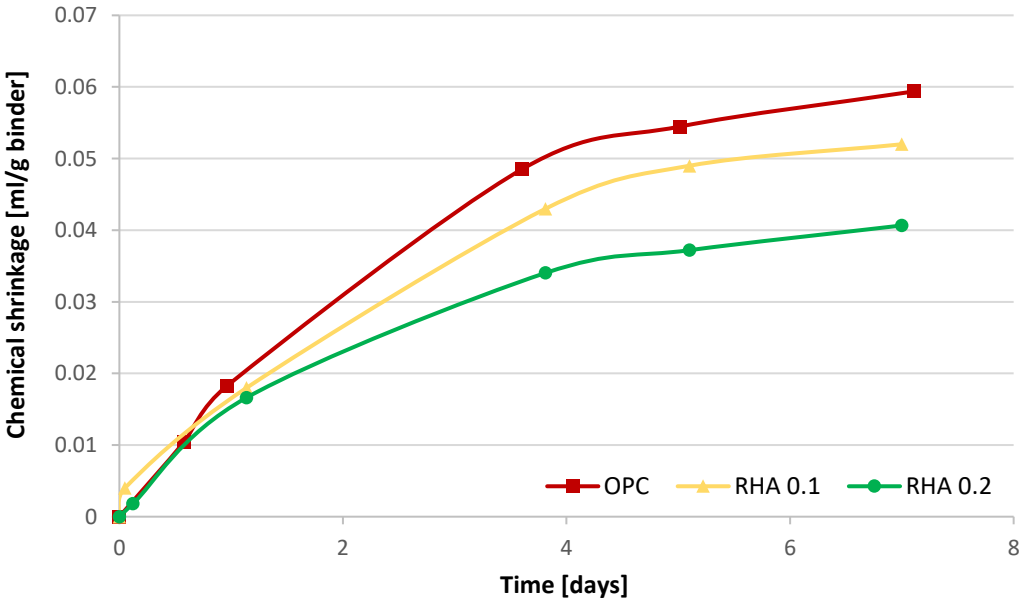

Figure 6

Accepted manuscript doi:
10.1680/jadcr.24.00078

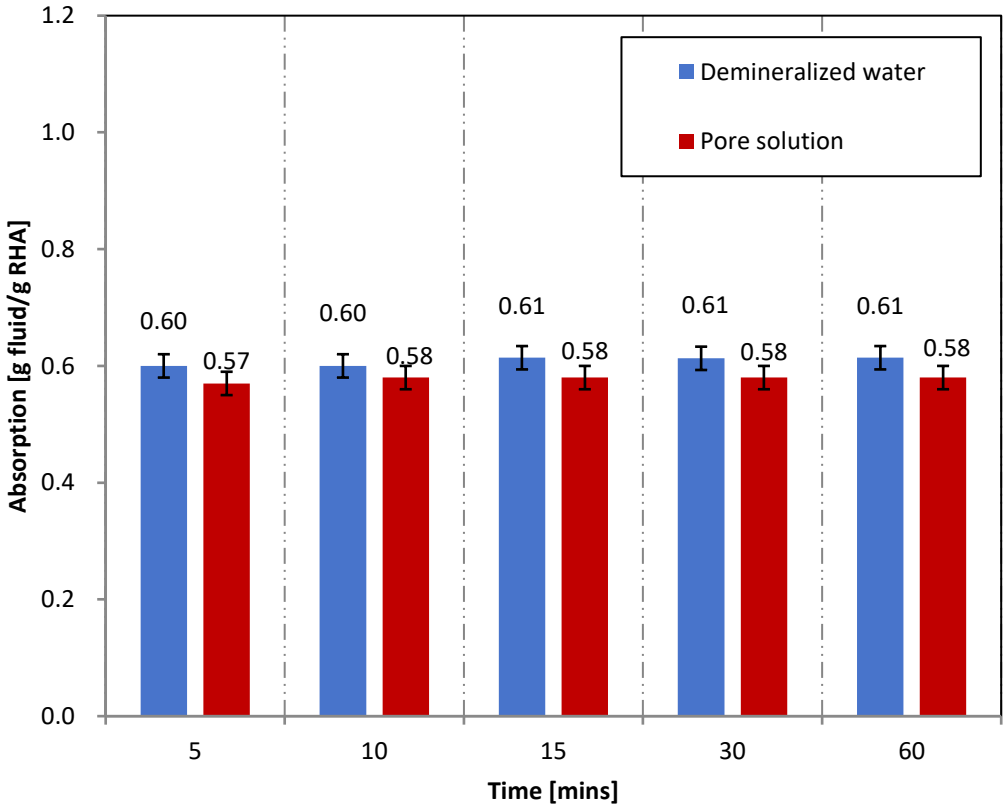

Figure 7

Accepted manuscript doi:
10.1680/jadcr.24.00078

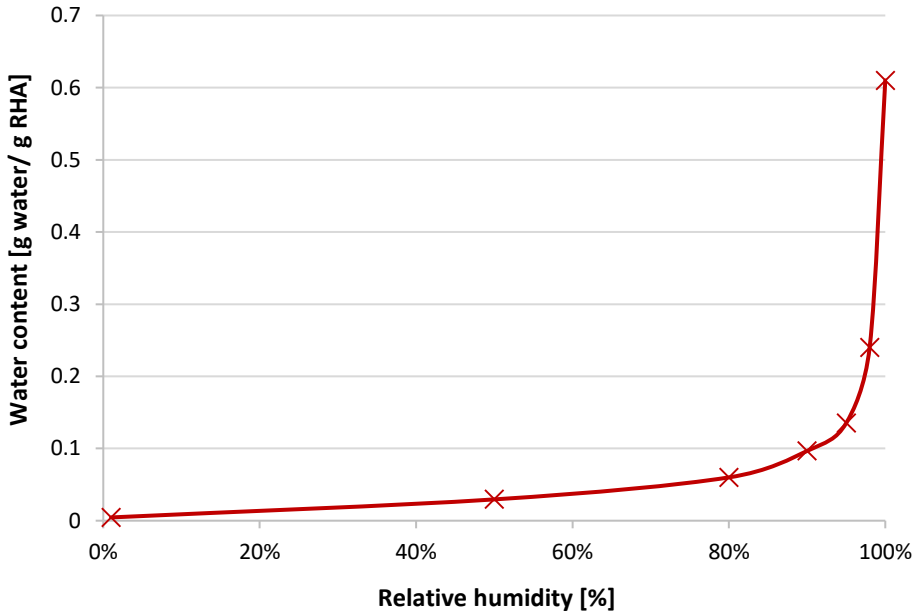

(a)

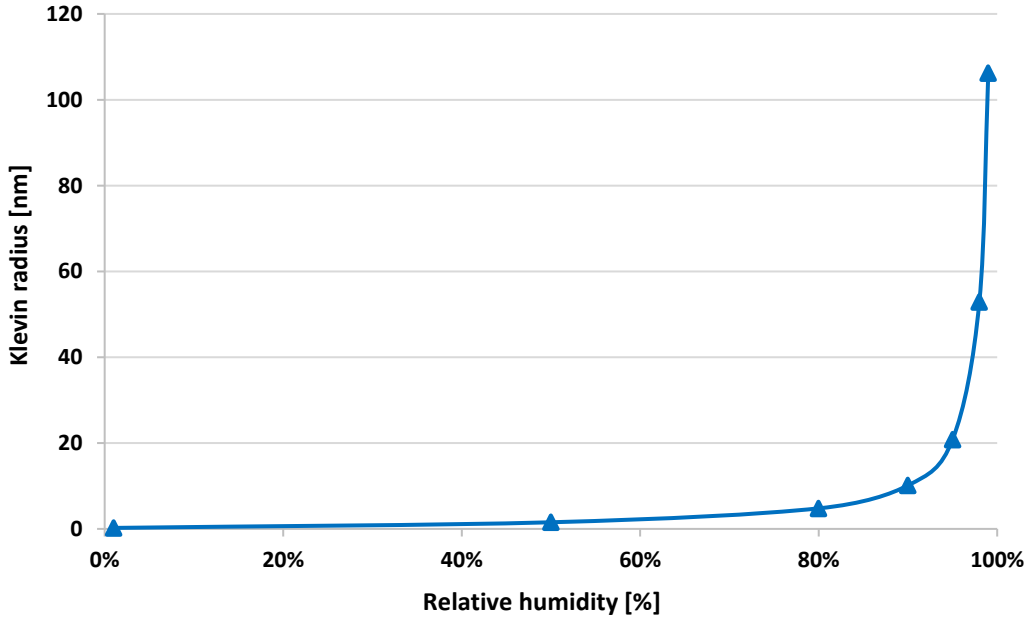

(b)

Figure 8

Accepted manuscript doi:
10.1680/jadcr.24.00078

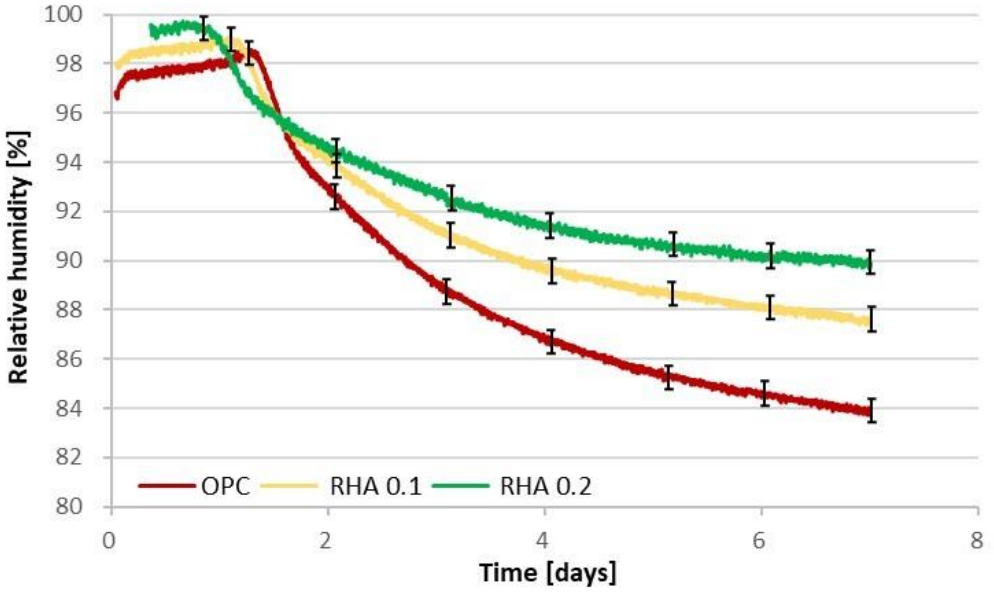

Figure 9

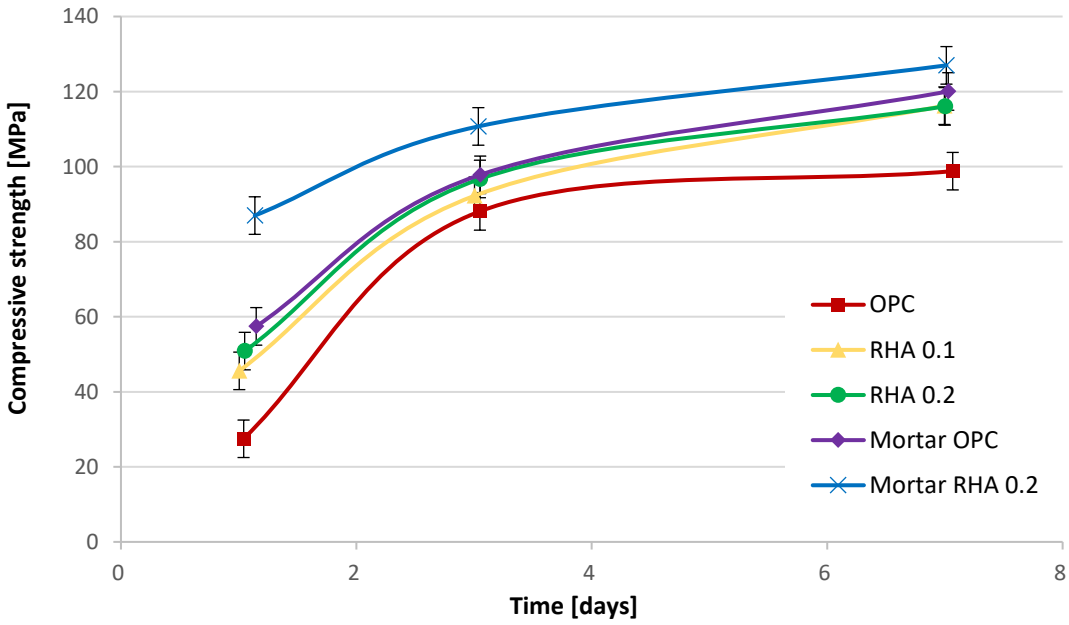

Figure 10

Accepted manuscript doi:
10.1680/jadcr.24.00078

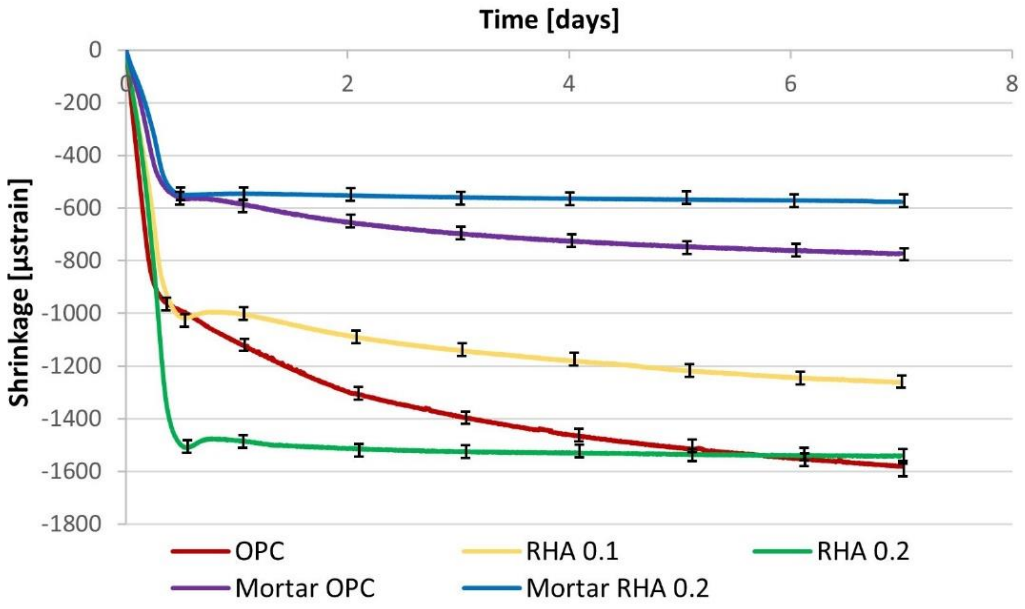

Figure 11

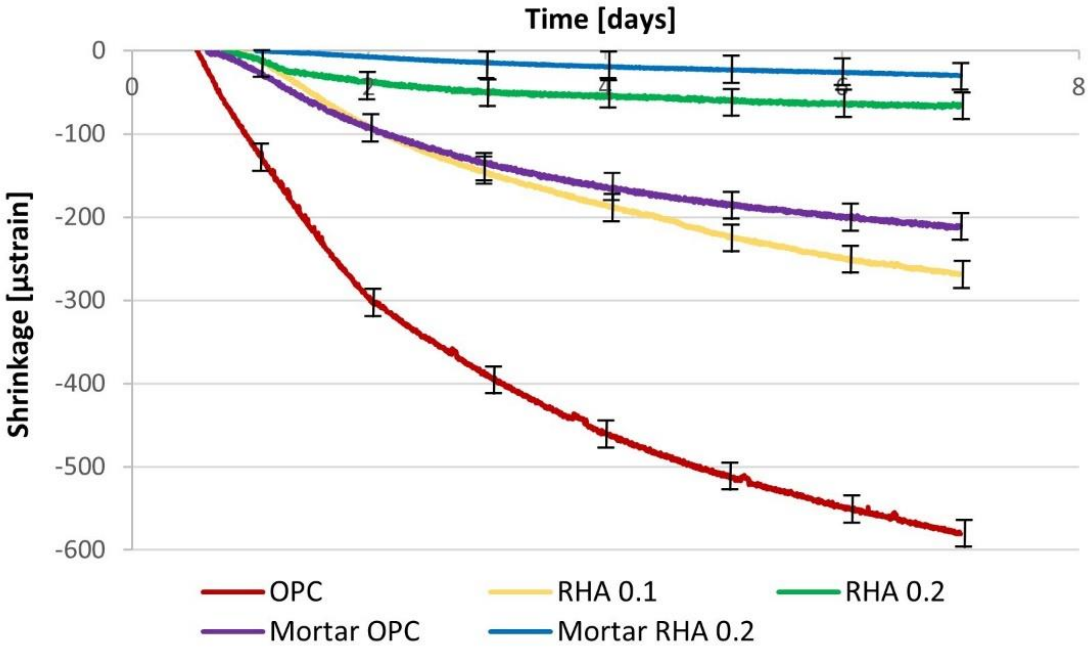

Figure 12

Accepted manuscript doi:
10.1680/jadcr.24.00078

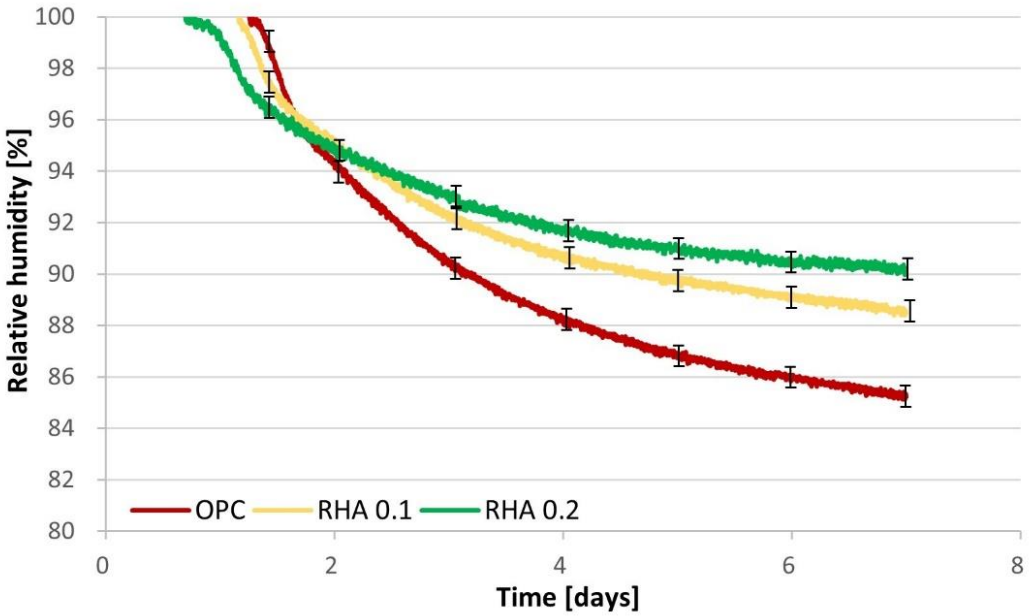

Figure 13

Accepted manuscript doi:
10.1680/jadcr.24.00078

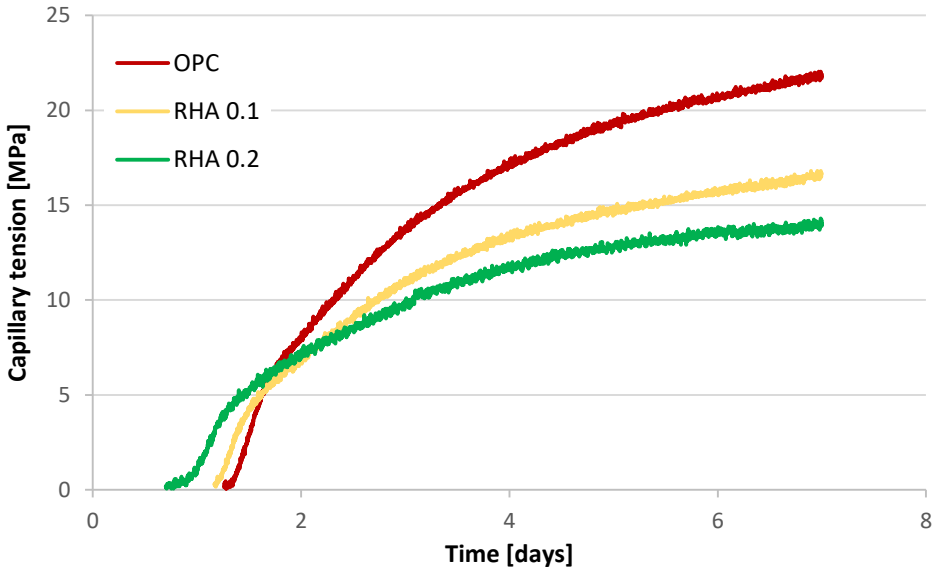

(a)

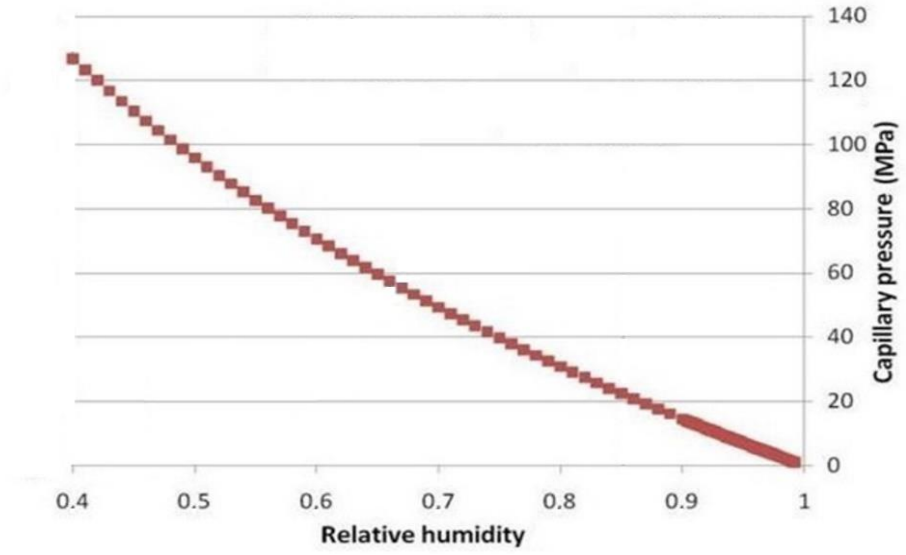

(b)

Figure 14

Accepted manuscript doi:
10.1680/jadcr.24.00078

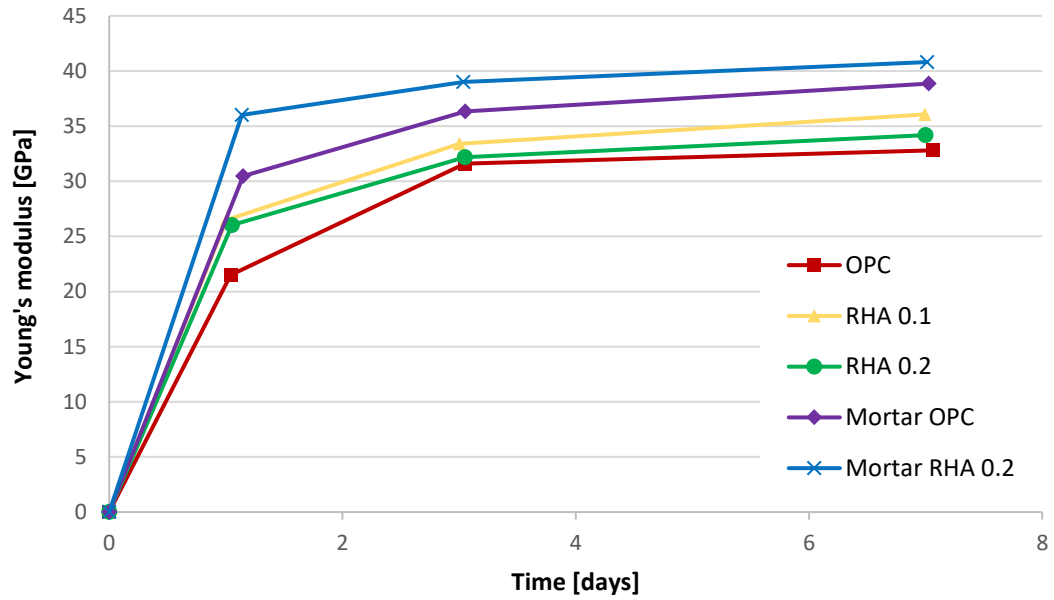

Figure 15

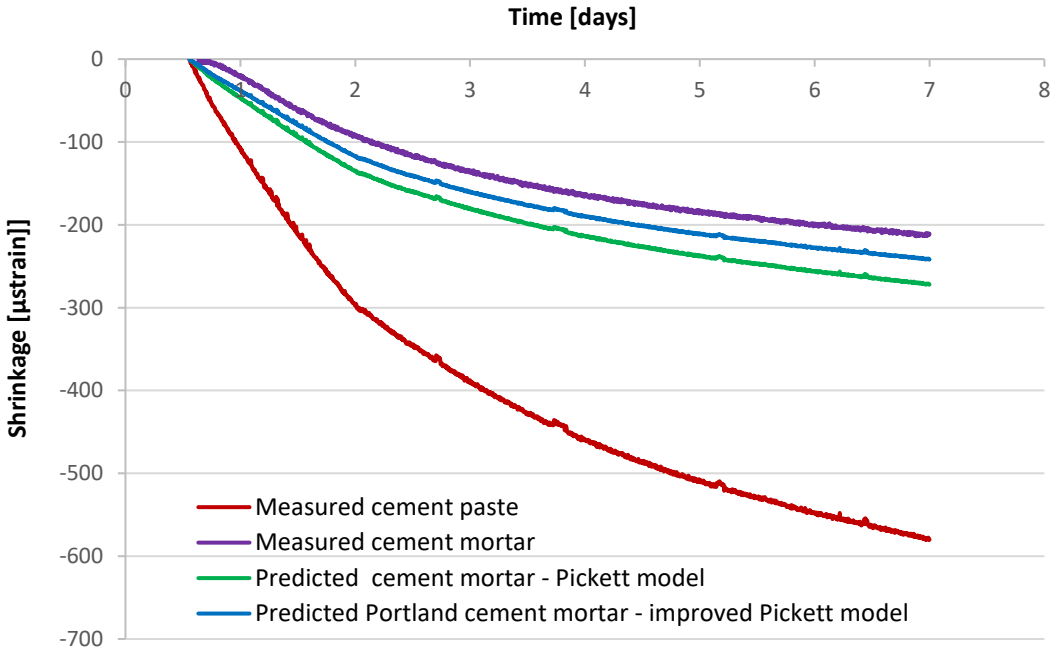

Figure 16

Accepted manuscript doi:
10.1680/jadcr.24.00078

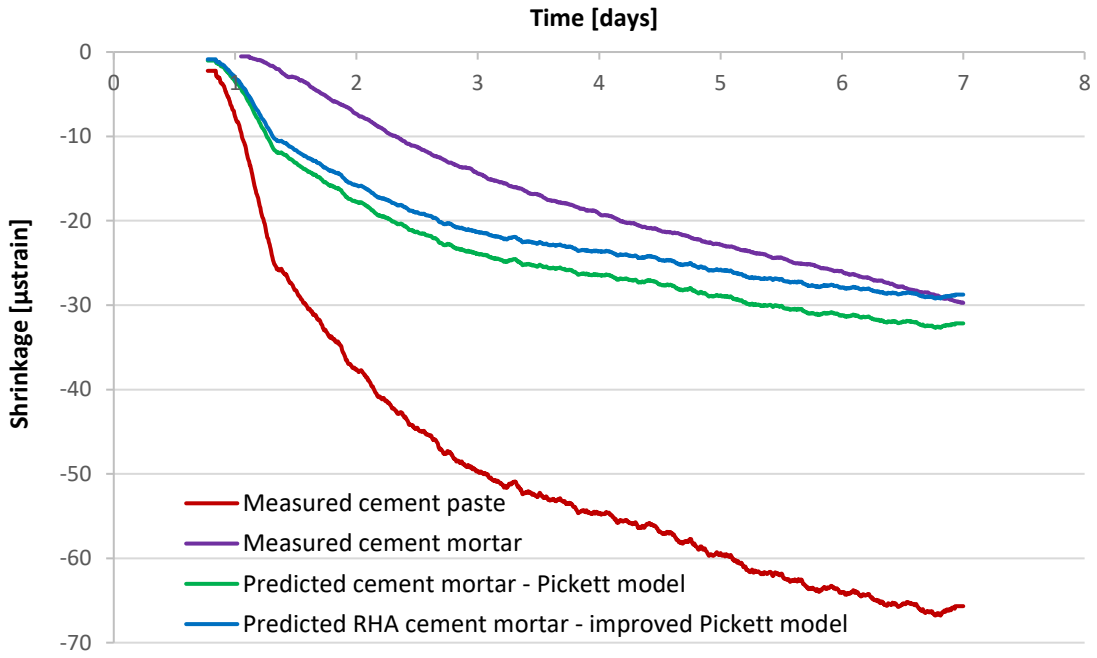

Figure 17

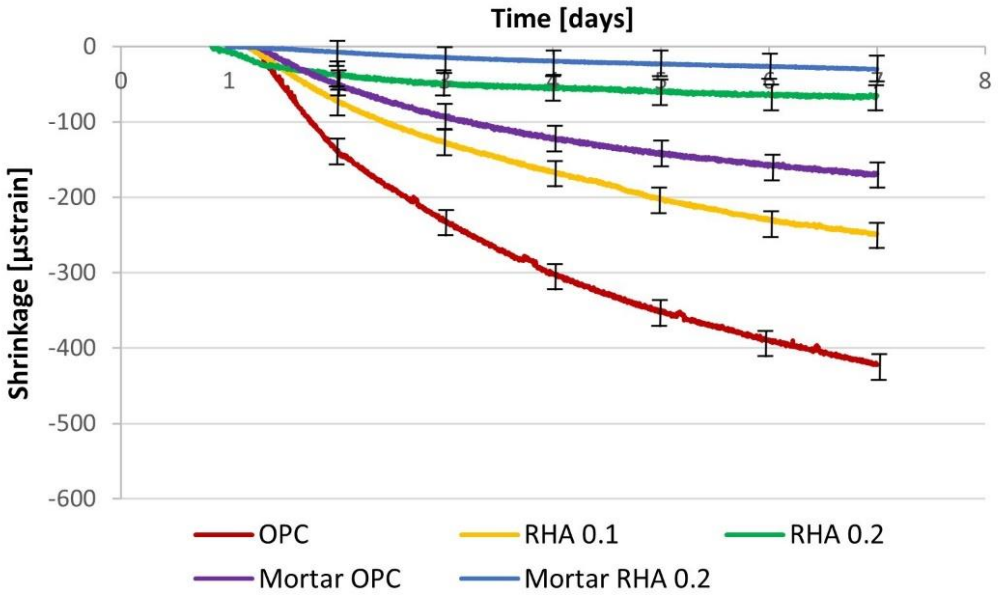

Figure 18

Accepted manuscript doi:
10.1680/jadcr.24.00078

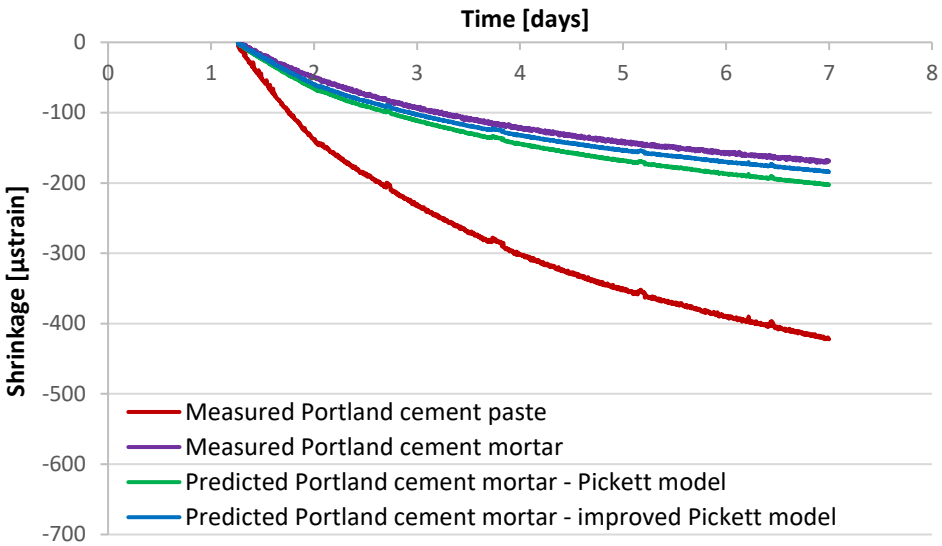

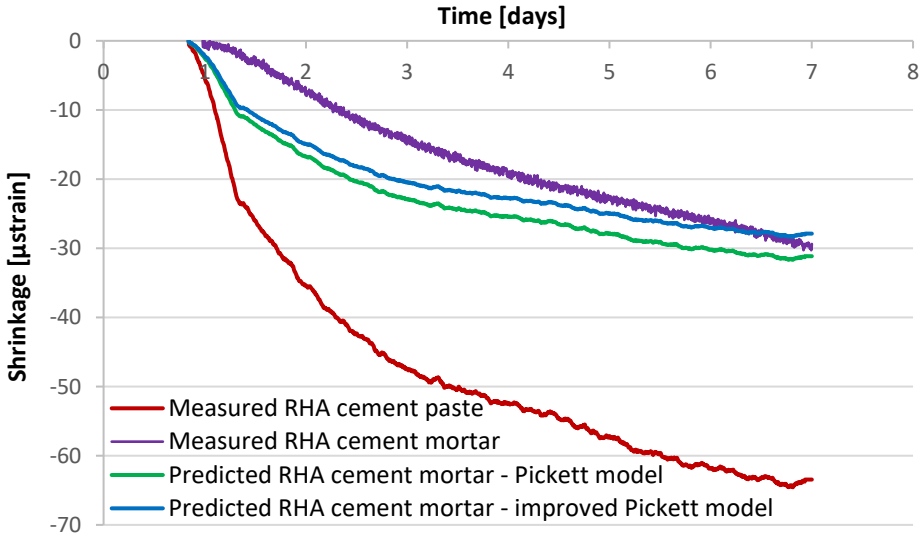

Figure 19